

Vivianite as an important iron phosphate precipitate in sewage treatment plants

Wilfert, P.; Mandalidis, A.; Dugulan, A. I.; Goubitz, K.; Korving, L.; Temmink, H.; Witkamp, G. J.; Van Loosdrecht, M. C M

DOI

[10.1016/j.watres.2016.08.032](https://doi.org/10.1016/j.watres.2016.08.032)

Publication date

2016

Document Version

Accepted author manuscript

Published in

Water Research

Citation (APA)

Wilfert, P., Mandalidis, A., Dugulan, A. I., Goubitz, K., Korving, L., Temmink, H., Witkamp, G. J., & Van Loosdrecht, M. C. M. (2016). Vivianite as an important iron phosphate precipitate in sewage treatment plants. *Water Research*, 104, 449-460. <https://doi.org/10.1016/j.watres.2016.08.032>

Important note

To cite this publication, please use the final published version (if applicable).
Please check the document version above.

Copyright

Other than for strictly personal use, it is not permitted to download, forward or distribute the text or part of it, without the consent of the author(s) and/or copyright holder(s), unless the work is under an open content license such as Creative Commons.

Takedown policy

Please contact us and provide details if you believe this document breaches copyrights.
We will remove access to the work immediately and investigate your claim.

Accepted Manuscript

Vivianite as an important iron phosphate precipitate in sewage treatment plants

P. Wilfert, A. Mandalidis, A.I. Dugulan, K. Goubitz, L. Korving, H. Temmink, G.J. Witkamp, M.C.M. Van Loosdrecht



PII: S0043-1354(16)30632-7

DOI: [10.1016/j.watres.2016.08.032](https://doi.org/10.1016/j.watres.2016.08.032)

Reference: WR 12303

To appear in: *Water Research*

Received Date: 23 May 2016

Revised Date: 8 August 2016

Accepted Date: 18 August 2016

Please cite this article as: Wilfert, P., Mandalidis, A., Dugulan, A.I., Goubitz, K., Korving, L., Temmink, H., Witkamp, G.J., Van Loosdrecht, M.C.M., Vivianite as an important iron phosphate precipitate in sewage treatment plants, *Water Research* (2016), doi: 10.1016/j.watres.2016.08.032.

This is a PDF file of an unedited manuscript that has been accepted for publication. As a service to our customers we are providing this early version of the manuscript. The manuscript will undergo copyediting, typesetting, and review of the resulting proof before it is published in its final form. Please note that during the production process errors may be discovered which could affect the content, and all legal disclaimers that apply to the journal pertain.

1 *Vivianite as an important iron phosphate precipitate in sewage*
2 *treatment plants*

3 P. Wilfert^{a,b}, A. Mandalidis^a, A.I. Dugulan^c, K. Goubitz^c, L. Korving^{a,*}, H. Temmink^{a,d}, G.J.
4 Witkamp^b and M.C.M Van Loosdrecht^b

5 ^aWetsus, European Centre Of Excellence for Sustainable Water Technology, Oostergoweg 7,
6 8911 MA, Leeuwarden, The Netherlands

7 ^bDept. Biotechnology, Delft Univ Technol, Van der Maasweg 9, 2629 HZ Delft, The Netherlands

8 ^cFundamental Aspects Mat & Energy Grp, Delft Univ Technol, Mekelweg 15, 2629 JB Delft, The
9 Netherlands

10 ^dSub-department of Environmental Technology, Wageningen University, P.O. Box 8129, 6700
11 EV Wageningen, The Netherlands

12 *Corresponding author: Phone: +31-58-2843160; e-mail: Leon.Korving@Wetus.nl

13 Abbreviations

14 CPR – Chemical Phosphorus Removal

15 COD – Chemical Oxygen Demand

16 DO - Dissolved Oxygen

17 DOC - Dissolved Organic Carbon

18 EBPR – Enhanced Biological Phosphorus Removal

19 Fe₂O₃ – Hematite

20 FeP - Iron Phosphorus Compounds

21 FeS_x - Iron Sulphide Compounds

22 IRB - Iron Reducing Bacteria

23 o-P - Orthophosphate

24 SRT – Solid Retention Time

25 STP – Sewage Treatment Plant

26 TS - Total Solids

27 Abstract

28 Iron is an important element for modern sewage treatment, inter alia to remove phosphorus from
29 sewage. However, phosphorus recovery from iron phosphorus containing sewage sludge, without
30 incineration, is not yet economical. We believe, increasing the knowledge about iron-phosphorus
31 speciation in sewage sludge can help to identify new routes for phosphorus recovery. Surplus and
32 digested sludge of two sewage treatment plants was investigated. The plants relied either solely on
33 iron based phosphorus removal or on biological phosphorus removal supported by iron dosing.
34 Mössbauer spectroscopy showed that vivianite and pyrite were the dominating iron compounds in
35 the surplus and anaerobically digested sludge solids in both plants. Mössbauer spectroscopy and
36 XRD suggested that vivianite bound phosphorus made up between 10 and 30 % (in the plant
37 relying mainly on biological removal) and between 40 and 50 % of total phosphorus (in the plant
38 that relies on iron based phosphorus removal). Furthermore, Mössbauer spectroscopy indicated
39 that none of the samples contained a significant amount of Fe(III), even though aerated treatment
40 stages existed and although besides Fe(II) also Fe(III) was dosed. We hypothesize that
41 chemical/microbial Fe(III) reduction in the treatment lines is relatively quick and triggers
42 vivianite formation. Once formed, vivianite may endure oxygenated treatment zones due to slow
43 oxidation kinetics and due to oxygen diffusion limitations into sludge flocs. These results indicate

44 that vivianite is the major iron phosphorus compound in sewage treatment plants with moderate
45 iron dosing. We hypothesize that vivianite is dominating in most plants where iron is dosed for
46 phosphorus removal which could offer new routes for phosphorus recovery.

47 Keywords:

48 Iron, Phosphorus, Sewage, Sewage sludge, Mössbauer spectroscopy, Vivianite

49 1 Introduction

50 Phosphorus (P) is an essential element for all life. It is often a limiting nutrient for crops and thus
51 a crucial part of fertilizers. Currently, the use of P is not sustainable and its supply is not
52 guaranteed in the future: (I) Phosphate rock reservoirs, the main source of P for fertilizers, are
53 depleting (Scholz and Wellmer, 2016; Walan et al., 2014), (II) these reservoirs are located in a
54 few countries (De Ridder et al., 2012), (III) for current P applications and depletions regional
55 imbalances exist (Macdonald et al., 2011; van Dijk et al., 2016) and (IV) P surpluses cause
56 eutrophication in surface waters (Carpenter, 2008). The recovery of P from secondary resources
57 would help to make its use in our society circular and more sustainable (Carpenter and Bennett,
58 2011; Childers et al., 2011).

59 Sewage is an important secondary source for P (van Dijk et al., 2016). In sewage treatment plants
60 (STPs), P is typically removed to diminish eutrophication in surface waters by chemical P
61 removal (CPR) or enhanced biological P removal (EPBR). In both cases, P is concentrated in the
62 sewage sludge. Iron (Fe) dosing for CPR is efficient, simple and cheap (Geraarts et al., 2007; Paul
63 et al., 2001; WEF, 2011). Future energy producing STPs rely on chemical P and chemical oxygen
64 demand (COD) removal (Böhnke, 1977; Wilfert et al., 2015). Additionally, Fe is commonly

65 applied in modern sewage treatment also for other reasons than CPR. Ferric, Fe(III) and ferrous,
66 Fe(II) iron salts are dosed as flocculants to remove COD (Li, 2005), to prevent the emission of
67 hydrogen sulphide (H₂S) in sewer systems and digesters (Hvitved-Jacobsen et al., 2013; Nielsen et
68 al., 2005) and to improve sludge dewatering (Higgins and Murthy, 2006). Additionally, Fe may
69 originate from groundwater intrusion into the sewer systems (Hvitved-Jacobsen et al., 2013;
70 Kracht et al., 2007). Thus, in most STPs, part of the P will be bound to Fe. An economic feasible
71 recovery of P from sewage sludge containing iron phosphorus compounds (FeP), without sludge
72 incineration, is a technological challenge that remains unsolved, also due to scarce information on
73 FeP mineralogy in STPs (Wilfert et al 2015).

74 The initial reactions, after Fe(III) or Fe(II) addition to sewage and the subsequent removal of P are
75 complex (El Samrani et al., 2004; Luedecke et al., 1989; Smith et al., 2008; Takács et al., 2006).
76 These reactions are important as they drive primary P removal from sewage by bringing P from
77 the liquid to the solid phase. In STPs, the solid retention time (SRT) can be a few hours, as in the
78 A-stage of AB-processes (Böhnke, 1977; Böhnke et al., 1997), but it is usually on the time scale
79 of 5-20 days when the conventional activated sludge process is applied (Tchobanoglous et al.,
80 2013). In those processes, alternating redox conditions are applied to achieve COD and nitrogen
81 removal. Hence, once formed the initial FeP may change due to oxidation of Fe(II) or reduction of
82 Fe(III) respectively (Nielsen, 1996; Nielsen et al., 2005; Nielsen and Nielsen, 1998; Rasmussen
83 and Nielsen, 1996) or due to aging effects (Recht and Ghassemi, 1970; Szabó et al., 2008). Most
84 likely, the FeP, that end up in the surplus sludge and that determine the P removal efficiency of
85 STPs, differ from the initial precipitates.

86 Several researchers reported the ferrous iron phosphate mineral vivianite (Fe(II)₃[PO₄]₂· 8H₂O) in
87 surplus sludge and anaerobically digested sludge (Frossard et al., 1997; Ghassemi and Recht,

88 1971; Seitz et al., 1973; Singer, 1972). Frossard et al., 1997 were able to quantify vivianite in
89 sewage sludge using Mössbauer spectroscopy even though the sludge samples in this study were
90 exposed to air. This could have resulted in full/partial oxidation of Fe(II) compounds and partial
91 transformation of vivianite to amorphous FeP (Roldan et al., 2002) or to other changes of the P
92 fractions (Kraal et al., 2009). Additionally, all Mössbauer measurements were done at room
93 temperature (300 K). Complex samples should ideally be measured at lower temperatures (e.g.
94 4.2 K) as well, to reveal unambiguously the spectral contributions and magnetic properties of the
95 Fe phases. (Murad and Cashion, 2004).

96 We have investigated two STPs, with different treatment strategies to determine the fate of Fe and
97 FeP during treatment. The STP Leeuwarden applies EBPR, additionally respectively Fe(II) or
98 Fe(III) are dosed in two different treatment lines. The STP Nieuwveer uses the AB technology
99 (Böhnke et al., 1997; De Graaff et al., 2015), here Fe(II) is dosed. AB-plants in combination with
100 cold anammox have the potential to be energy factories (Jetten et al., 1997; Siegrist et al., 2008).

101 The fate of Fe and FeP was evaluated by various measurements on the liquid and solid fractions of
102 the sewage (sludge) at different locations in the treatment line. Mössbauer spectroscopy
103 (qualitative and quantitative analyses of Fe compounds), XRD (semi-quantitative analyses of all
104 crystalline material) and SEM-EDX (particle morphology and elemental composition) were used
105 to characterize the solid fractions. Mass balances for P and Fe helped to identify the significance
106 of different sources (influent, external sludge, Fe dosing) and sinks (effluent, sludge disposal) for
107 these elements. Mössbauer spectroscopy and XRD were used to estimate P bound in vivianite and
108 sulphide extraction was used to quantify P bound to Fe. Thereby, the P recovery potential of a
109 technology that targets specifically on FeP was determined.

110 Identifying the forms of FeP in activated sludge would help to obtain thermodynamic (e.g.
111 equilibrium concentrations) and stoichiometric (molar Fe:P ratios) information that is necessary to
112 develop technologies to recover P from FeP. Although, in literature, some indications for vivianite
113 formation as major P compound during sewage treatment can be found, the role of vivianite and
114 its importance has been neglected, the reason why this study was carried out.

115 2 Methods & Material

116 2.1 STPs and sampling

117 In the AB plant Nieuwveer (influent: $75706 \text{ m}^3 \text{ d}^{-1}$ in 2014), Fe(II) is added in the aerated
118 ($\approx 0.3 \text{ mg dissolved oxygen (DO) L}^{-1}$) A-stage for P and COD removal. SRTs are 15 hours in the
119 A-stage, 16 days in the B-stage (DO in aerated sections $\approx 1.8 \text{ mg DO L}^{-1}$) and 25 days during
120 anaerobic digestion. In the EBPR plant Leeuwarden ($38,000 \text{ m}^3 \text{ d}^{-1}$ in 2014), the influent is split in
121 two treatment lines (60 % of the sewage goes to Line 1). Besides for CPR, Fe is dosed to prevent
122 H_2S emissions into the biogas during anaerobic digestion. In Line 1, Fe(III) is dosed and in Line 2
123 Fe(II) is dosed in the nitrification zone ($\approx 1.5 \text{ mg DO L}^{-1}$). SRTs before digestion are around 15
124 days (50 % in the aerated zone) and during anaerobic digestion around 42 days. The digesters of
125 both STPs, receive external sludge which accounts for about 30 % (Nieuwveer) and about 25 %
126 (Leeuwarden) of the total digested sludge. At both locations, samples were taken to analyse the
127 composition of the of the sewage (sludge). From these measurements (Table A. 1 and Table A. 2)
128 Fe and P mass balances were calculated. To calculate Fe and P loads, average daily flow rates of
129 the sampling days were used. Samples were taken between December 2014 and March 2015, after
130 a period of 48 h without precipitation. The STP Leeuwarden was sampled three times. Results

131 reported in Table A. 1 and for the mass balances are average values of the triplicate measurements
132 and of the daily loads of these samplings. The STP Nieuwveer was sampled once in March 2015.

133 Samples were stored and transported in cooling boxes on ice to reduce microbial activity. Sample
134 processing started 1 h (Leeuwarden) and 3 h (Nieuwveer) after sampling. Sample drying started
135 latest 8 h after sampling and was completed within 24 h. Sampling and sample processing were
136 done under anaerobic conditions to prevent oxidation and degassing of samples. Sewage was
137 collected; using syringes with attached tubing that were washed several times with sewage.

138 Sewage sludge was taken from valves using a funnel with attached tubing. Samples were then
139 filled in serum bottles. To rinse bottles, about three times their volume was flowed through the
140 bottle by inserting the end of the tubing to the bottom of the bottle. Then the bottles were sealed
141 with butyl rubber stoppers (referred to as anaerobic samples hereafter). With these samples the
142 composition of the liquid phase was determined and material for solid analyses was obtained. For
143 total solids (TS), volatile solids (VS) and to determine the total elemental composition of the
144 sewage (sludge), separate samples, without special pre-cautions to prevent sample oxidation, were
145 taken (hereafter, referred to as mass balance (MB) samples). Separate sampling was considered to
146 be necessary as the TS content of the anaerobic samples could change due to rinsing of serum
147 bottles.

148 In Nieuwveer, the influent sample was a mixture of raw influent and recirculated effluent (40 % of
149 the effluent is recirculated). For the mass balances, the Fe and P concentrations of the raw effluent
150 were calculated. The external sludge sample was taken from a pre-storage tank, and contained an
151 unknown mixture of external sludge. In Leeuwarden, P loads from external sludge were below the
152 detection limit and had to be calculated from the difference in P loads before and after digestion.

153 2.2 Analyses

154 Oxidation-Reduction Potential (ORP), pH and conductivity were measured potentiometrically in
155 the plants. Total elemental composition of MB samples were determined after microwave assisted
156 acid digestion ($\text{HNO}_3=69\%$, 15 min, $180\text{ }^\circ\text{C}$) followed by ICP-OES. Total solids and VS were
157 measured according to standard methods (APHA, AWWA, WEF, 1998). For total alkalinity
158 measurements, 10 mL MB sample was titrated to $\text{pH}=4.5$ with 0.1 N HCl (APHA, AWWA, WEF,
159 1998).

160 The anaerobic samples were transferred into plastic centrifuge tubes inside an anaerobic glovebox
161 ($95\% \text{ N}_2/5\% \text{ H}_2$, $\text{O}_2<10$ ppm) and centrifuged (15 min, 3200 G). Dissolved elemental
162 compositions (ICP-OES), dissolved anions (IC) and dissolved organic carbon, DOC (LC-OCD)
163 were determined after filtration of the supernatant ($0.45\text{ }\mu\text{m}$) inside the glovebox. Dissolved
164 Fe(II)/Fe(III) was determined in the filtrate using the ferrozine method according to Viollier et al.,
165 2000. In short, an appropriate sample volume was added to $100\text{ }\mu\text{L}$ ferrozine reagent and made up
166 to a total volume of $1100\text{ }\mu\text{L}$ using Milli-Q water. After 15 minutes the absorbance of the
167 ferrozine-Fe(II) complex was recorded. Subsequently, to reduce all Fe(III) to Fe(II), $150\text{ }\mu\text{L}$ of a
168 1.4 mol L^{-1} hydroxylamine solution was added to $800\text{ }\mu\text{L}$ of this solution. The reduction time was
169 12 h ($30\text{ }^\circ\text{C}$) to make sure that organic complexed Fe(III) was completely reduced (Rasmussen and
170 Nielsen, 1996; Verschoor and Molot, 2013). Eventually, $50\text{ }\mu\text{L}$ of an 10 mol L^{-1} ammonium
171 acetate buffer solution was added and the absorbance was again measured. With these information
172 the Fe(II) and Fe(III) concentration can be calculated. All ferrozine measurements were confirmed
173 by measuring total Fe by ICP-OES. Additionally, Fe(II)/Fe(III) stock solutions were added to
174 filtrates to test the reliability of the photometric measurements (Table 1). For sulphide (S^{2-})

175 measurements, samples were filtered inside the glovebox into a zinc acetate solution (0.8 M),
176 stored in the dark and measured after 24 h by the methylene blue method (Cline, 1969).

177 Solid material was derived from centrifuge pellets of the anaerobic samples. Inside the glovebox,
178 pellets were finely spread on glass plates, dried (25 °C, 24 h, in the dark) and grinded using a
179 mortar and pestle. Vivianite can be found when samples are dried at room temperature, even in
180 the presence of oxygen. Higher temperatures for sample drying should be avoided. Above 70 °C,
181 in the presence oxygen, vivianite is transformed within hours into an amorphous iron phosphate
182 compound (Čermáková et al., 2015). Thus, in such sludge samples, vivianite disappears (Poffet,
183 2007).

184 Samples for XRD analyses were filled in glass capillaries and sealed first with modelling clay and
185 then superglue. Right before analyses, glass capillaries were sealed using a burner. The
186 measurements were done on a PANalytical X'Pert PRO diffractometer with Cu-K α radiation (5-
187 80 °2 θ , step size 0.008°). The results from XRD analyses were made semi-quantitative by
188 determining the amorphous and crystalline peak area of the spectra (Origin Pro 9). This allows the
189 determination of the degree of crystallinity and thus of the total mineral share of the sample. All
190 samples that were analysed by Mössbauer spectroscopy were also analysed by XRD. In addition,
191 two samples that were sampled in the aerated treatment lines (referred to as A-stage and Line 2
192 activated sludge samples) were analysed using XRD.

193 For Mössbauer analyses, samples were filled in plastic rings, sealed with Kapton tape and super
194 glue and then wrapped in parafilm. It was expected that considerable amounts of P are bound in
195 vivianite, thus a vivianite standard was prepared according to Roldan et al., 2002. Transmission
196 ⁵⁷Fe Mössbauer spectra were collected at 4.2 and 300 K with conventional constant-acceleration

197 and sinusoidal velocity spectrometers using a $^{57}\text{Co}(\text{Rh})$ source. Velocity calibration was carried
198 out using an $\alpha\text{-Fe}$ foil. The Mössbauer spectra were fitted using Mosswin 4.0 (Klencsár, 1997).
199 Morphology and elemental compositions of sludge particles in the grinded solids was also
200 analysed by SEM-EDX. Samples for SEM-EDX were exposed to air during measurements.

201 Extractability of Fe in digested sludge was investigated using water, to extract water soluble Fe
202 (pH=7, Wolf et al., 2009). Na-pyrophosphate solution (0.1 mol L^{-1} , pH=9.5) was used to extract
203 and quantify organic bound Fe. Pyrophosphate was used to extract organic bound Fe and Fe
204 minerals mainly in soil but also from sewage sludge, vivianite was partially dissolved with this
205 extract (Carliell-Marquet et al., 2009; McKeague, 1967; van Hullebusch et al., 2005). With
206 pyrophosphate extraction no distinction between Fe(II)/Fe(III) could be made. Ammonium
207 oxalate (0.2 mol L^{-1} $\text{NH}_4\text{-oxalate}$, pH=3) extracts poorly crystalline Fe, it was used to determine
208 Fe(II)/Fe(III) in activated sludge before (Rasmussen and Nielsen, 1996). Each extraction was
209 done in separate butyl rubber stoppered serum bottles, the extracts were added to wet sludge
210 (n=3). Oxygen in the extracts was removed using headspace gas exchange equipment with a gas
211 mixture containing 70 % N_2 and 30 % CO_2 in 5 cycles. The extract:TS ratios were 100:1 for H_2O
212 and pyrophosphate and 1000:1 for oxalate. All samples were shaken in the dark (16 h, $30 \text{ }^\circ\text{C}$,
213 100 rpm) before analysing Fe in the filtered ($0.45 \text{ }\mu\text{m}$) but not centrifuged extracts.

214 2.3 Estimate P bound to Fe

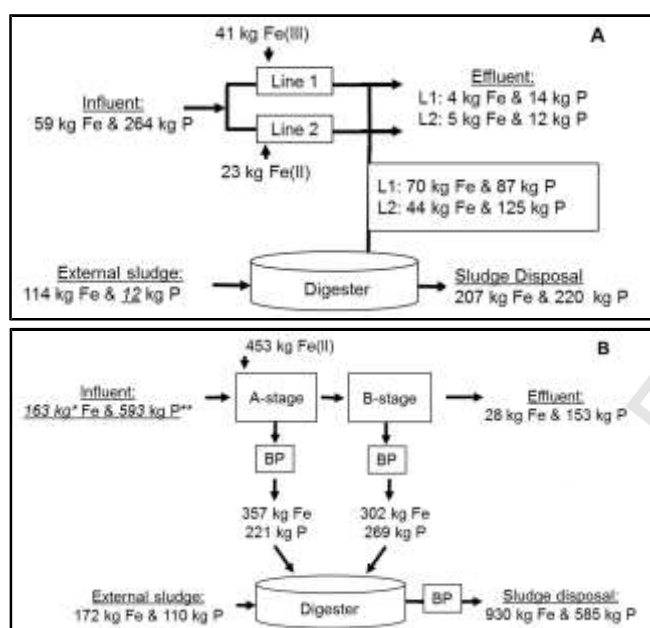
215 P bound in vivianite was calculated from results of semi-quantitative XRD and Mössbauer
216 spectroscopy. Additionally, to determine sulphide extractable P, 0.5 molar Na_2S solution was
217 added to 2 L digested sludge (molar Fe:P=0.55) and surplus sludge from Line 1 (molar
218 Fe:P=0.25) from Leeuwarden and to digested sludge from Nieuwveer (molar Fe:P =0.73) in molar
219 ratios $\text{S}^{2-}:\text{Fe}$ of 1.5. These samples were taken several months before/after the other samples. For

220 Leeuwarden, molar Fe:P were very similar to the sludge used for other analyses, digested sludge
221 showed an Fe:P=0.56 and Line 1 an Fe:P=0.28 but for Nieuwveer the sludge for the sulphide
222 experiments had a lower Fe:P (0.73 vs 0.89). It was assumed that sulphide extracts specifically P
223 bound to FeP (Kato et al., 2006). The experiments were done in a gastight reactor with pH control
224 (pH=7.5) with a reaction time of at least 24 h. Samples from the reactor were taken using N₂
225 flushed syringes, filled in N₂ rinsed plastic centrifuge tubes under a stream of N₂ and centrifuged
226 (15 min, 3200 G). Subsequently, sulphide, ortho-P (o-P) and the elemental composition were
227 determined in samples that were filtered using N₂ flushed syringes and filters (0.45 µm). At the
228 end of these experiments at least 1 mmol sulphide L⁻¹ was still in solution indicating that the
229 extraction was not sulphide limited. The maximum amounts of P that could be bound to Fe, Mg
230 and Al were quantified by using the elemental composition of the TS (Table A. 1 & Table A. 2).
231 For these calculations it was assumed that all solid Mg is present as struvite (molar Mg:P =1), all
232 Fe as vivianite (molar Fe:P=1.5) and Al as a precipitate with a molar Al:P of 1.5 (Hsu, 1976).

233 3 Results

234 3.1 Mass balances

235 In the STP Leeuwarden, mass balances showed, that the influent Fe load equals approximately the
236 dosed Fe (Figure 1A). The effluent load was approximately 15 % of the influent Fe and 10 % of
237 the influent P. The solid molar Fe:P ratio almost doubles from 0.33 before to 0.57 after anaerobic
238 digestion due to digestion of external sludge with a high Fe (8.4 g Fe /kg sludge) and low P (not
239 detectable) content. About 95 % of the external sludge originates from two cheese factories which
240 use Fe(III) as flocculent.



241
242
243
244
245
246
247 *Figure 1: Daily mass balances for Fe and P in the STPs Leeuwarden (A) and Nieuwveer (B). Underlined*
248 *numbers were calculated (BP = belt press).*

249 For Nieuwveer, the mass balance showed that, dosed Fe is about three times the Fe entering via
250 the influent (Figure 1B). The effluent load was 15 % of the influent Fe and 25 % of the influent P.
251 The Fe and P loads from the A and B stage to the anaerobic digestion are similar. During
252 digestion, the molar Fe:P ratio increased, due to external sludge, from 0.76 to 0.89.

253 The mass balances were established by a single sampling campaign in Nieuwveer and three
254 sampling campaigns in Leeuwarden. It was not intended to make a comprehensive mass balance
255 which would require several samplings throughout the year. The mass balance served to identify
256 main Fe sources and sinks in the STPs. For Nieuwveer, the calculated P loads of the influent,
257 effluent and into the digester were about 20 % higher, the external sludge P input about 20 %
258 lower when compared to the average yearly P loads for 2014 which were determined from daily P
259 measurements on pooled samples (number from yearly balance/from our balance): influent (460
260 vs 593 kg P d⁻¹), effluent (118 vs 153 kg P d⁻¹), external sludge (139 vs 110 kg P d⁻¹) and to the
261 digester (411 vs 490 kg P d⁻¹). Since loads (except for the external sludge) were consistently

262 higher for our measurements it can be assumed that patterns of Fe and P loads represent typical
263 situations for the STP. For Leeuwarden, average yearly P loads in 2014 in the influent were also
264 about 20 % higher (318 vs 264 kg P d⁻¹) and almost the same for the effluent (28 vs 26 kg P d⁻¹).
265 Phosphorus flows into the digester are not regularly determined in Leeuwarden.

266 The maximum gap for the mass balance was about 15 % for Fe in the STP Nieuwveer, mainly
267 caused by an excess of Fe leaving the digester. In contrast, the gap in the P mass balance was only
268 5 %. The gap in the Fe balance is most likely due to the lack of a representative external sludge
269 sample. In Nieuwveer, external sludge is delivered in irregular intervals from various STPs
270 applying CPR (Al/Fe dosing) and EBPR respectively. The external sludge sample in Nieuwveer
271 was taken from a storage tank that, most likely, contained sludge also from a non Fe dosing plant.
272 This explained why we underestimate Fe input into the digester whereas the P loads can be traced
273 back.

274 3.2 Dissolved Fe(II)&Fe(III)

275 Fe(II)/Fe(III) stock solutions were added (n=3) to filtrates, obtained from digested sludge and
276 from surplus sludge of Line 1 in Leeuwarden, to test the reliability of the ferrozine method (Table
277 1). In filtrates from surplus sludge, Fe(II) was overestimated by about 7 % and Fe(III) by about
278 4 %. In filtrates from digested sludge Fe(II) was added. Here, Fe(II) was underestimated by 2 %
279 and Fe(III) overestimated by about 5 %. When Fe(III) was added it was overestimated by about 1
280 %. These results indicate that the method can reliably detect dissolved Fe(II) and Fe(III) in
281 sewage samples.

282 After digestion, dissolved Fe in Leeuwarden sludge was surprisingly dominated by Fe(III), 1.6 mg
283 L⁻¹ (Table 1). Also in digested sludge in Nieuwveer about half of the dissolved Fe was detected as

284 Fe(III), 3.0 mg L⁻¹. In general, dissolved Fe in most samples was dominated by Fe(III). This
285 Fe(III) could be free Fe(III) or Fe(III) which was complexed by organic ligands such as humic
286 substances (Table 1, Buffle, 1990).

287 Although standard addition was successful, the results should, especially after digestion, be
288 regarded with some caution. Fe(II)/Fe(III) were determined reliably, even in the presence of
289 dissolved organic matter (DOM, 16–25 mg DOC L⁻¹) using the ferrozine method (Verschoor and
290 Molot, 2013; Viollier et al., 2000). However, Viollier et al., 2000, added Fe(III) only. Verschoor
291 and Molot, 2013 found Fe(II) and Fe(III) successfully back. Yet, when added, Fe(II) could be
292 present as free Fe(II), whereas the Fe(II) that was already in the sample could partly also be
293 present in complexed forms (Buffle, 1990). In surplus sludge, dissolved organic matter was on the
294 same order of magnitude (Nieuwveer A-stage: 15 mg DOC L⁻¹, Leeuwarden Line 1: 20 mg DOC
295 L⁻¹) compared to the successful standard additions described before. In digested sludge, DOC
296 concentrations were much higher, in Nieuwveer, 320 mg DOC L⁻¹ and in Leeuwarden, 126 mg
297 DOC L⁻¹.

298 With the ferrozine assay, as we applied it, only free Fe(II) was detected (Jackson et al., 2012).
299 When part of the Fe(II) was complexed by DOM, it was not detected in our first step, in which
300 Fe(II) is quantified. Subsequently, to determine Fe(III), the sample pH was lowered, a reducing
301 agent was added and the sample incubated (12 h). Under these conditions, complexed Fe(II) is
302 mobilized and could be incorrectly assigned to Fe(III) (Gaffney et al., 2008; Jackson et al., 2012,
303 Rasmussen and Nielsen, 1996). That also explains why total Fe levels from ICP-OES and from
304 the ferrozine measurements matched very well. With ICP-OES free and complexed Fe is detected.
305 To measure free and total Fe(II) in the samples the method of Gaffney et al., 2008 could be
306 established for sewage samples. Additionally, a complementary method to determine Fe

307 speciation e.g. by voltammetry would help to eliminate analytical uncertainties (Buffle, 1990). In
308 Leeuwarden, samples from Lines 1 and 2 and from the influent were on-site filtered and directly
309 added in Ferrozine to test if free Fe(II) is present, no colour reaction was visible.

310 Despite all efforts, it cannot be excluded that part of the Fe(II) was oxidized during sampling or
311 sample processing due to high sensitivity of Fe(II) to oxygen (Verschoor and Molot, 2013).

312 Subsequently, total dissolved Fe concentrations may decrease due to precipitation of ferric iron
313 oxides. Ferrous iron can even get microbial oxidized in absence of oxygen (Nielsen and Nielsen,
314 1998). An opposing mechanism, that could occur after sampling and during sample transport, is
315 the conversion of solid Fe(III) oxides to soluble Fe(II) by iron reducing bacteria (IRB).

316 Accordingly, dissolved Fe(II) concentrations doubled within 24 h in samples from the A-stage and
317 B-stage in Nieuwveer when they were incubated at 30 °C (data not shown).

318 Classifying complexed Fe(II) as Fe(III) by the ferrozine assay and oxygen contamination, could
319 explain the presence of dissolved Fe(III) after the anaerobic digestion. From a chemical point of
320 view all dissolved Fe should be present as Fe(II). During anaerobic digestion, highly reducing
321 conditions, including the formation of strong reducing agents like sulphide, prevail for more than
322 three weeks. Also others found significant amounts of dissolved Fe(III) after similar periods of
323 anaerobic incubation (Cheng et al., 2015). An increase of the oxidation-reduction potential over
324 time could indicate that anaerobic conditions did not prevail in these experiments. In our
325 discussion we will focus on total dissolved iron levels instead of the oxidation state of the
326 dissolved Fe.

327

Table 1: Dissolved Fe(II) and Fe(III) measurements from STPs Leeuwarden and Nieuwveer

	ID	Fe(II) mg L ⁻¹	Fe(III) mg L ⁻¹	Fe (total) mg L ⁻¹
Leeuwarden	Surplus sludge Line 1, Fe(III)	0.1	0.5	0.6
	Activated sludge Line 2, Fe(II)	0.1	0.5	0.6
	Surplus sludge Line 2, Fe(II)	0.6	0.6	1.1
	Digested sludge	0.6	1.6	2.1
Nieuwveer	A-stage: after FeII dosing	0.0	0.8	0.8
	A-stage: Surplus Sludge	18.3	12.7	31.0
	B-stage: Surplus Sludge	0.0	1.9	1.9
	Digested sludge	2.9	3.0	5.9
Standard addition	Filtrate (undigested) + Fe(II): 11.8 mg L ⁻¹	12.7 (±0.24)	0	12.7
	Filtrate (undigested) + Fe(III): 11.1 mg L ⁻¹	0	11.6 (±0.0)	11.6
	Filtrate (digested) + Fe(II): 11.3 mg L ⁻¹	11.1 (±0.08)	0.6 (±0.14)	11.7
	Filtrate (digested) + Fe(III): 10 mg L ⁻¹	0	10.1 (±0.5)	10.1

328

329 3.3 Solids

330 3.3.1 XRD

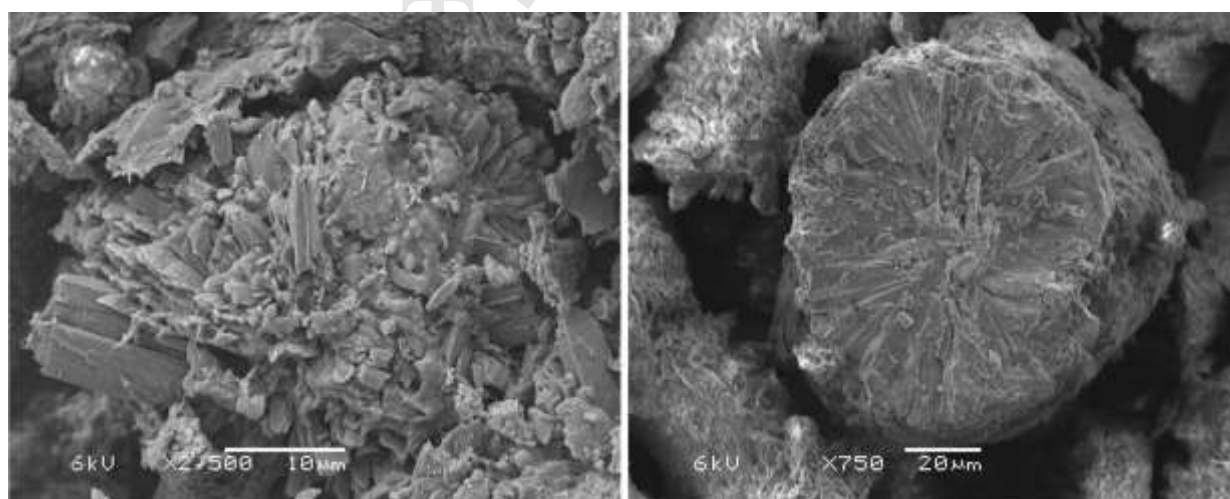
331 XRD analyses revealed that vivianite and quartz were present in all samples (all XRD
332 diffractograms and peak assignments are included in the supporting information). In the STP
333 Leeuwarden, struvite was the dominating crystalline P phase (Table 2). During anaerobic
334 digestion the relative share of struvite decreases compared to quartz and vivianite. In the STP
335 Nieuwveer vivianite, as the only P containing crystalline phase, was detected in all samples. In
336 digested solids and both A-stage samples from Nieuwveer, a peak at around 29.4 °2 θ with
337 intensities between 3.9 and 8.6 % could not be assigned.

338 *Table 2: Results of semi quantitative XRD and VS analyses expressed as % of the total solids.*

	Sampling station	Quartz (%)	Vivianite (%)	Struvite (%)	XRD amorphous (%)	VS (%)
Leeuwarden	Line 1, Fe(III): Surplus sludge	7	2	11	80	70
	Line 2, Fe(II): Activated sludge	7	3	10	79	66
	Line 2, Fe(II): Surplus sludge	6	3	7	84	68
	Digested sludge	21	6	11	63	62
Nieuwveer	A-stage: Activated Sludge	10	7	0	83	78
	A-stage: Surplus Sludge	8	6	0	86	80
	B-stage: Surplus Sludge	11	8	0	81	78
	Digested sludge	11	8	0	63	60

340 3.3.2 SEM-EDX

341 In both STPs, no large particles with an overlap of Fe and P were found before the anaerobic
 342 digestion using SEM-EDX. Iron and P were homogenously distributed in the samples. After
 343 anaerobic digestion larger FeP particles (between 20 and 150 μm in diameter) with different
 344 crystalline morphologies were found (Figure 2). These particles showed Fe:P ratios between 1.1
 345 and 1.7 when measured by EDX.

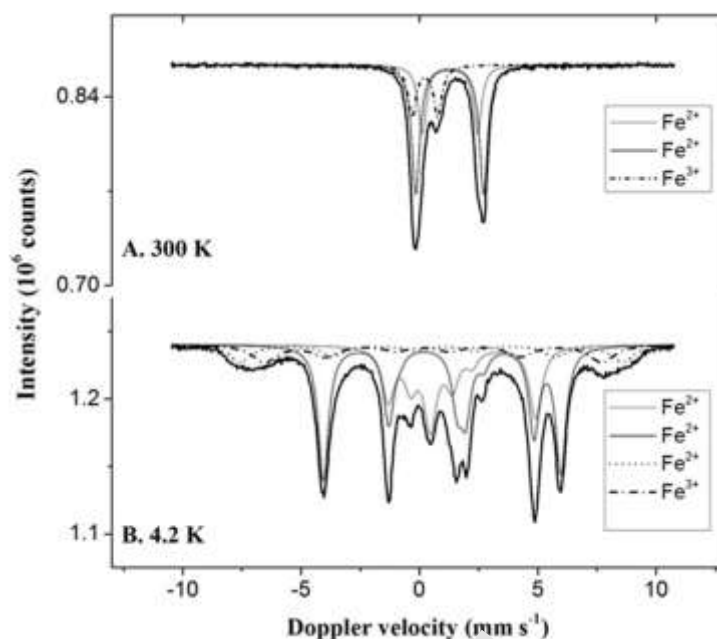


346
 347 *Figure 2: SEM images of particles in digested sludge solids sampled in Leeuwarden (left) and Nieuwveer*
 348 *(right). EDX showed Fe:P ratios between 1.1 (Leeuwarden) and 1.7 (Nieuwveer).*

349 3.3.3 Mössbauer spectroscopy

350 Results of Mössbauer measurements at 4.2 K are summarized in Table 3 (all spectra and
351 measurements at 300 K are included in the supporting information). Mössbauer spectroscopy at
352 liquid helium temperature is more powerful as it reveals unambiguously the oxidation states and
353 magnetic properties of the different Fe structures. The samples from Leeuwarden with digested
354 solids and the vivianite standard showed signs of oxidation (25 to 28 % of vivianite was oxidized
355 in the standard and in digested sludge respectively). Before measurements, these samples were
356 sealed followed by storage at ambient atmosphere inside glass bottles with screw caps for about 1
357 month. Subsequently, other samples were stored inside the glovebox until measurement and no
358 signs of oxidation were visible, as indicated by the absence of oxidized vivianite.

359 The spectra acquired with the vivianite standard (Figure 3) showed that about 75 % of the
360 vivianite was not affected by oxidation and allowed to obtain a spectrum with parameters that are
361 in good agreement with the literature for the two Fe(II) sites (Gonser and Grant, 1976). The
362 oxidized magnetically split Fe(III) species in this standard might be an intermediate valence state
363 between Fe(III) and Fe(II) like in magnetite (Harker and Pollard, 1993). Others suggested that
364 oxidation of vivianite results in the formation of amorphous FeP (Miot et al., 2009), Lepidocrocite
365 (Roldan et al., 2002) or lipscombite, beraunite or rockbridgite (Leavens, 1972).



366
 367 *Figure 3: Mössbauer spectra obtained at different temperatures with the vivianite standard.*
 368 Samples taken from Line 1, Fe(III) dosing and Line 2, Fe(II) dosing in Leeuwarden were virtually
 369 the same. Between 94 and 96 % of the total Fe was Fe(II). Iron in vivianite represented 36 and 32
 370 % of the total Fe in Lines 1 and 2 respectively. The significant (33 and 35 %) paramagnetic
 371 contribution to the spectra which was not magnetically split at 4.2 K was assigned to Fe(II) in
 372 pyrite, FeS₂. All other Fe species in these samples (summing up to about 30 %) could not be
 373 decisively assigned. Mössbauer spectra of a digested sludge sample taken in Leeuwarden to which
 374 sulphide was added contained the unknown Fe(II) compound that was still paramagnetic at 4.2 K
 375 (data not shown as this sample was exposed to oxygen), which contributed 20-21 % to the total Fe
 376 pool in the samples from Lines 1 and 2. Thus, we assumed this very well defined compound ($\Gamma =$
 377 0.4 mm s^{-1}) is a sulphur phase. However, many iron sulphide (FeS_x) and iron sulphate compounds
 378 can be excluded as they are magnetic split at 4.2 K or because they have different Mössbauer
 379 parameters (Mullet et al., 2002; Sklute et al., 2015; Yoshida and Langouche, 2013). The presence
 380 of FeP minerals cannot be excluded (Dyar et al., 2014), for instance, the Mössbauer parameters of

381 anapaite, $\text{Ca}_2\text{Fe}^{2+}(\text{PO}_4)_2 \cdot 4\text{H}_2\text{O}$ are close to the values we obtained (Eeckhout et al., 1999).

382 Overall, we cannot assign this spectra to a certain Fe phase. The Fe(III) phase is an iron oxide
383 possibly hematite, Fe_2O_3 (Murad and Cashion, 2004).

384 The spectra obtained for the digested sludge sample in Leeuwarden showed that vivianite was the
385 only FeP present (73 %). About 28 % of Fe comes from oxidized vivianite and 45 % of the Fe
386 from vivianite unaffected by oxidation. The remaining 27 % of Fe(II) in this sample was pyrite.

387 In the samples from the STP Nieuwveer, Fe(II) dominated as well. The samples contained
388 vivianite, pyrite, an Fe(III) having Mössbauer parameters resembling those of hematite, Fe_2O_3
389 (Murad and Cashion, 2004) and a paramagnetic (doublet) Fe(II) species that might be assigned to
390 vivianite. The isomer shift of this Fe(II) is close to the one of vivianite, and the quadrupole
391 splitting is also consistent with paramagnetic vivianite. Our measurements were made close to the
392 Neel temperature (magnetic ordering temperature) of vivianite (12 K). It could be that some
393 dispersed vivianite structures or vivianite structures with impurities are still paramagnetic at 4.2
394 K. The quantification of vivianite using XRD suggested that this unknown Fe(II) is vivianite
395 (Table 4). However, this Fe(II) could also be vivianite overlapping with another phase; as well as
396 it can be another Fe compound other than vivianite. In the surplus sludge of the A-stage about 69
397 % of the Fe was present as vivianite, additional 18 % as the potential vivianite phase, 9 % as
398 pyrite and 4 % as Fe_2O_3 . The Fe in the surplus sludge sampled from the B-stage was assigned to
399 vivianite (55 %), to the potential vivianite phase (33 %), pyrite (7 %) and to Fe_2O_3 (5 %). In
400 digested solids, 54 % of the Fe could be firmly assigned to vivianite, 27 % were assigned to the
401 potential vivianite phase, the share of pyrite was (15 %) and the remaining Fe (4 %) was assigned
402 to Fe_2O_3 . For the subsequent discussions, it was assumed that the Fe(II) species that could not
403 clearly be assigned to vivianite with Mössbauer spectroscopy was in fact vivianite.

404 In all samples from Nieuwveer and in digested sludge from Leeuwarden no iron phosphate
 405 minerals besides vivianite were present. In surplus sludge from Leeuwarden the presence of other
 406 FeP phases than vivianite, cannot be excluded. Only, minor fractions of P can be adsorbed to the
 407 Fe_2O_3 .

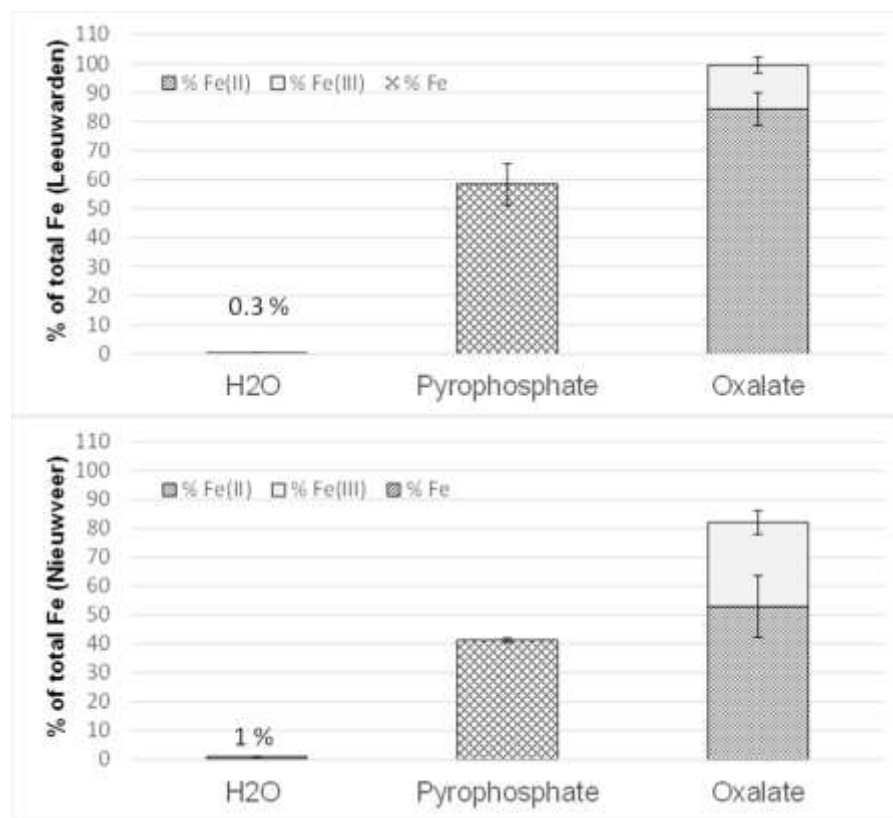
408 *Table 3: Results of Mössbauer measurements at 4.2 K. Experimental uncertainties: Isomer shift (IS): \pm*
 409 *0.01 mm s^{-1} ; Quadrupole splitting (QS): $\pm 0.01 \text{ mm s}^{-1}$; Line width (Γ): $\pm 0.01 \text{ mm s}^{-1}$; Hyperfine field: \pm*
 410 *0.1 T ; Spectral contribution: $\pm 3\%$.*

Sample	IS ($\text{mm}\cdot\text{s}^{-1}$)	QS ($\text{mm}\cdot\text{s}^{-1}$)	Hyperfine field (T)	Γ ($\text{mm}\cdot\text{s}^{-1}$)	Phase	Spectral contribution (%)
Leeuwarden Surplus Sludge Line 1: (Fe(III)) dosing	0.27	0.88	-	0.84	Fe^{2+} Pyrite	33
	0.37	0.05	51.8	0.58	Fe^{3+} Fe_2O_3	6
	0.93	-	19.3	0.74	Fe^{2+}	5
	1.29	2.47	-	0.47	Fe^{2+}	20
	1.01	1.00	11.4	1.07	Fe^{2+} Vivianite I	14
	1.26	3.71	24.8	1.07	Fe^{2+} Vivianite II	22
Leeuwarden Surplus Sludge Line 2: (Fe(II)) dosing)	0.29	0.84	-	0.87	Fe^{2+} Pyrite	35
	0.37	-0.20	51.4	0.58	Fe^{3+} Fe_2O_3	4
	1.07	-	24.7	0.77	Fe^{2+}	8
	1.31	2.48	-	0.46	Fe^{2+}	21
	1.01	0.61	11.4	1.07	Fe^{2+} Vivianite I	15
	1.11	3.37	26.4	1.07	Fe^{2+} Vivianite II	17
Leeuwarden digested solids	0.42	0.79	-	0.72	Fe^{2+} Pyrite	27
	0.50	-0.84	46.0	1.41	Fe^{3+} Oxidized	15
	0.71	0.81	46.3	1.41	Fe^{2+} vivianite	13
	1.20	0.50	10.0	1.18	Fe^{2+} Vivianite I	24
	1.25	2.70	26.7	1.18	Fe^{2+} Vivianite II	21
Nieuwveer Surplus sludge A-stage	0.27	1.00	-	0.92	Fe^{2+} Pyrite	9
	0.38	-0.19	51.9	0.86	Fe^{3+} Fe_2O_3	4
	1.21	2.79	-	0.79	Fe^{2+} Dispersed vivianite	18
	1.22	2.27	15.0	0.64	Fe^{2+} Vivianite I	21
	1.21	3.13	26.4	0.64	Fe^{2+} Vivianite II	48
Nieuwveer Surplus sludge B-stage	0.33	0.88	-	0.87	Fe^{2+} Pyrite	7
	0.37	-0.14	49.8	0.86	Fe^{3+} Fe_2O_3	5
	1.16	2.92	-	0.92	Fe^{2+} Dispersed vivianite	33
	1.26	2.23	14.9	0.93	Fe^{2+} Vivianite I	18
	1.18	3.32	26.2	0.93	Fe^{2+} Vivianite II	37
Nieuwveer Digested solids	0.33	0.88	-	0.87	Fe^{2+} Pyrite	15
	0.37	0.20	48.9	0.86	Fe^{3+} Fe_2O_3	4
	1.21	2.86	-	1.23	Fe^{2+} Dispersed vivianite	27
	1.16	2.21	15.0	0.77	Fe^{2+} Vivianite I	15
	1.20	3.05	26.8	0.77	Fe^{2+} Vivianite II	39
Vivianite Standard	0.35	0.45	44.2	1.24	Fe^{3+} Oxidized	13
	0.77	-0.54	50.2	1.15	Fe^{2+} vivianite	12
	1.35	2.36	14.8	0.64	Fe^{2+} Vivianite I	29
	1.36	3.14	27.4	0.53	Fe^{2+} Vivianite II	46

411

412 3.3.4 Extractions

413 Water, pyrophosphate and ammonium oxalate were used to extract Fe from digested sludge
414 sampled in Leeuwarden (Figure 4A) and Nieuwveer (Figure 4B). Water was the mildest extract
415 and dissolved 0.3 and 1 % of the total solid Fe in Leeuwarden and Nieuwveer respectively. This
416 was expected, considering the relatively low solubility of FeS_x and vivianite that dominated the
417 digested sludge samples (Al-Borno and Tomson, 1994; Davison, 1991). However, in both STPs
418 about 60 % of the water extractable Fe was Fe(III). During pyrophosphate extraction all dissolved
419 Fe species were quantified, summing up to between 40 % (Nieuwveer) and 60 % (Leeuwarden) of
420 the Fe. Considering the Mössbauer measurements, Fe bound in pyrite or vivianite must be part of
421 this fraction. Thus, the Fe extracted using pyrophosphate was mainly of non-organic origin.
422 Pyrophosphate extracts rather Fe from vivianite than from FeS_x (Carliell-Marquet et al., 2009). In
423 Leeuwarden, the Fe fraction in pyrophosphate (58 ± 7 %) is in a similar range as vivianite (57 %,
424 Mössbauer spectroscopy). However, in Nieuwveer, the pyrophosphate extracted Fe (41 ± 1 %) was
425 much less than Fe bound in vivianite (81 %, Mössbauer spectroscopy). Ammonium oxalate
426 extracted from Leeuwarden digested sludge all Fe (85 % as Fe(II)) and around 80 % of the Fe in
427 Nieuwveer digested sludge (65 % as Fe(II)). Compared to the Mössbauer measurements, this
428 indicates that the oxalate extraction and subsequent spectrophotometric determination of
429 Fe(II)/Fe(III) overestimate the Fe(III) content by about 10 and 25 %. The described uncertainties
430 for the spectrophotometric measurements for dissolved Fe(II)/Fe(III) could also affect the results
431 of the Fe extraction.



432 *Figure 4: Extraction of Fe from digested sludge using different extracts. The error bars indicate standard*
 433 *deviation (n=3).*

434 3.3.5 P bound to FeP

435 The maximum amount of P bound that could be bound to Fe was estimated by using the elemental
 436 composition of the solids. Sulphide extraction was used to dissolve P bound to Fe. Phosphorus
 437 bound in vivianite was determined by semi-quantitative XRD and by Mössbauer spectroscopy
 438 (Table 4). The results for Leeuwarden indicate that in surplus sludge between 9 % (Mössbauer
 439 spectroscopy) and 13 % (XRD) and after digestion between 18 % (XRD) and 29 % (Mössbauer
 440 spectroscopy) of the P is bound in vivianite. According to XRD, the majority of P was bound in
 441 struvite in surplus (43 %) and digested sludge (35 %). These values are higher than the maximum
 442 values obtained from the elemental compositions. Thus, semi quantitative XRD overestimated the
 443 struvite content in the sludge.

444 In the A-stage and the B-stage, estimates were in good agreement, about 50 % of the P in the A-
 445 stage and about 40 % of the P in the B-stage were bound in vivianite. After digestion, the
 446 estimates differ considerably between sulphide extraction (31 % of P bound to Fe) and Mössbauer
 447 spectroscopy and XRD (the latter two suggested 47 % and 53 % of the P are bound in vivianite).
 448 Additional, in Nieuwveer and Leeuwarden a maximum of 25 and 8 % of the total P could be
 449 bound to Al respectively.

450 Table 4 indicates that, the elemental compositions of the samples tends to overestimate P bound to
 451 Fe as it does not take into account non Fe-FeP species (e.g. iron oxides, FeS_x or organic bound
 452 Fe). The same principle applies in estimating P bound to Mg in struvite or to Al in aluminium
 453 phosphorus compounds (AlP). XRD may underestimate P bound to Fe as only the P bound to
 454 vivianite is detected. Also Mössbauer spectroscopy may underestimate P bound to Fe as not all
 455 compounds were identified and as the Fe_2O_3 can bind P.

456 *Table 4: Estimating P bound to FeP in different sewage (sludge) samples (n.d. = not determined).*

Leeuwarden	Average Line 1 & 2		Digested Sludge			
	% of total P		% of total P			
	Vivianite/FeP	Struvite/MgP	Vivianite/FeP	Struvite/MgP		
qXRD	13	43	18	35		
Mössbauer	9	-	29	-		
Elemental composition	26	36	36	25		
Sulfide	11	-	26	-		
Nieuwveer	A-stage Surplus sludge		B-stage Surplus Sludge		Digested Sludge	
	% of total P		% of total P		% of total P	
	Vivianite/FeP	Struvite/MgP	Vivianite/FeP	Struvite/MgP	Vivianite/FeP	Struvite/MgP
qXRD	54	0	37	0	53	0
Mössbauer	52	-	38	-	47	-
Elemental composition	55	15	43	14	59	14
Sulfide	n.d.	-	n.d.	-	31	-

458 4 Discussion

459 Significant Fe loads entered both STPs via the influent, which could originate from the municipal
 460 sewage itself, from groundwater infiltration and from Fe dosing into the sewer system (Hvitved-

461 Jacobsen et al., 2013; van den Kerk, 2005). This often neglected, but nevertheless, large Fe input
462 could assist in P removal in STPs (Gutierrez et al., 2010). Despite of its significant contribution,
463 the speciation of the influent Fe and whether it can support CPR or not was not determined. The
464 Fe dosing in both STPs (as for most other STPs in The Netherlands) was relatively low. The
465 molar ratios of Fe dosed to P entering via the influent was in Leeuwarden 0.13 and in Nieuwveer
466 0.42 (Figure 1). External Fe sources (i.e. influent and external sludge) contributed to about 80 %
467 of the total Fe in the STP Leeuwarden. Here, a large input of Fe via the external sludge into the
468 digester was identified. This suggests that Fe dosing can be significantly reduced, the external Fe
469 input is sufficient to prevent H₂S emissions during anaerobic digestion. In Nieuwveer, the dosed
470 Fe contributed more significantly to the total Fe budget, yet still 35 % of the total Fe load
471 originated from the inflowing sewage and from external sludge.

472 Dissolved Fe was measured to identify equilibrium concentrations with Fe compounds. However,
473 it turned out that during the dynamic conditions in the treatment lines of any STP (oxidizing and
474 reducing conditions coupled to high microbial activities) measuring of a static/equilibrium Fe
475 concentration is arbitrary. Thus, the reported dissolved Fe levels should be seen as an order of
476 magnitude for these zones. Except for the influent and effluent samples, by far most of the Fe is
477 part of the solid fraction. Accordingly, it was shown that even Fe(II), as product of IRB, can
478 remain part of the solid phase (Rasmussen and Nielsen, 1996). The high dissolved Fe
479 concentrations in the surplus sludge of the A-stage in Nieuwveer (about 30 mg Fe L⁻¹) highlighted
480 the possibility of a slow or insufficient Fe(II) oxidation resulting in small dispersed Fe(III) and
481 dissolved Fe(II). Sufficient oxidation and formation of Fe(III) oxides would cause a more rapid
482 precipitation compared to Fe(II) (Ghassemi and Recht, 1971; Oikonomidis et al., 2010).

483 Improving the aeration of Fe(II) or dosing of Fe(III) may help to improve the limited COD
484 removal in the A-stage of this STP (De Graaff et al., 2015).

485 The methodology which we employed for ammonium oxalate extraction gave only rough
486 estimates about the Fe(II)/Fe(III) content in the sludge. The pyrophosphate extraction did not
487 reliably extract organic Fe, as explained earlier (Stucki, 2013). In this study, Mössbauer
488 spectroscopy was the most reliable method for quantifying and identifying Fe and FeP
489 compounds. In contrast to XRD, Mössbauer spectroscopy can detect also amorphous Fe and FeP
490 phases with very small particle sizes in low abundances provided appropriate standards have been
491 prepared. On the other hand XRD detects all crystalline P compounds, also the ones that do not
492 contain Fe. Mössbauer spectroscopy and XRD collectively showed that the solid Fe compounds of
493 surplus sludge and anaerobic digested sludge were dominated by the ferrous phosphate mineral
494 vivianite. Ferric iron did not play a significant role in any of the solid samples. Besides vivianite,
495 the other major Fe compound was pyrite (Table 3).

496 In a membrane bioreactor with anoxic/aerobic zones, Fe(III) dominated the solid iron pool (Wu et
497 al., 2015) also in sludge sampled from the aeration tank of an STP using Fe(II) for CPR,
498 ammonium oxalate extraction showed that Fe(III) dominated (Rasmussen and Nielsen, 1996).
499 However, in our samples, regardless of aerobic zone in the STPs, Fe(II) was dominant.

500 How is that possible? First, despite aerated areas, the sludge itself is partly non-aerated e.g. during
501 low loading rates on weekends or in the night, in settlers and in the anoxic zones allowing the
502 reduction of Fe(III). In flocs, oxygen free conditions can prevail throughout the treatment process
503 due to diffusion limitation and when relatively low dissolved oxygen set-points are used. Thus,
504 once vivianite is formed, anoxic conditions in flocs may help to channel it, without oxidation,

505 through the aerated nitrification zone. Both, ours (SEM-EDX) and earlier research (Frossard et al.,
506 1997; Zelibor et al., 1988) showed that vivianite is often part of an organic matrix.

507 High activity of IRB in STPs has been measured which could result in rapid Fe(III) reduction and
508 thus vivianite production (Cheng et al., 2015; Rasmussen and Nielsen, 1996). Assuming the
509 reduction rates from Rasmussen and Nielsen, 1996, it would take between 19 h and 4 days in
510 Leeuwarden and between 24 h and 5 days in Nieuwveer to reduce all solid Fe in the surplus
511 sludge. These figures also indicate that Fe(III) reduction after sampling could influence the
512 oxidation state of the Fe in samples. Once vivianite is formed, its chemical oxidation is relatively
513 slow, on the time scale of weeks (Miot et al., 2009; Roldan et al., 2002). The oxidation by
514 anaerobic nitrate-reducing iron-oxidizing bacteria was faster: it took approximately 16 days for
515 complete oxidation (Miot et al., 2009). We could not find information on how long iron-oxidizing
516 bacteria in the presence of oxygen would need for the oxidation of Fe(II) in vivianite.

517 In Nieuwveer and in Line 2 in Leeuwarden, where Fe(II) is dosed for CPR, the mechanisms of
518 vivianite formation were not obvious. Vivianite could either directly precipitate from solution or
519 formed as a result of Fe(III) reduction. Indirect chemical Fe(III) reduction, induced by e.g.
520 sulphide, FeS_x or via humic substances (Biber et al., 1994; Golterman, 2001; Kappler et al., 2004)
521 or direct Fe(III) reduction by IRB (Azam and Finneran, 2014; Cheng et al., 2015; Nielsen, 1996;
522 Zhang, 2012) may have caused the formation of Fe(II) and subsequent precipitation of vivianite.
523 Vivianite could also be precipitated directly from solution as a result of Fe(II) dosing, possibly
524 combined with insufficient oxidation of Fe(II) (Ghassemi and Recht, 1971). In Line 1 in
525 Leeuwarden where Fe(III) is dosed, also most of the solid Fe was present as Fe(II), mainly as
526 vivianite. Here, chemical or biologically Fe(III) reduction must play a role. To what extent
527 vivianite forms already in the sewer systems cannot be determined by our measurements.

528 When Fe(III) is used for CPR, it was suggested that first Fe(III) oxides form which cause the P
529 removal via co-precipitation or adsorption (Smith et al., 2008). If the Fe:P ratio of these initial
530 ferric FeP is higher than the one of vivianite (molar Fe:P=1.5) as suggested before by Fulazzaky et
531 al., 2014 and Luedecke et al., 1989, then Fe(III) reduction and subsequent formation of vivianite
532 can act as a net sink for P. Hence, oxidation of Fe(II) in vivianite could result in P release due to a
533 higher molar Fe:P ratio in the formed products (Miot et al., 2009; Roldan et al., 2002). In case of
534 FeP with a molar Fe:P of 1 (e.g. strengite), Fe(III) reduction would cause a slight net P release.
535 However, more significant P release could only be expected when vivianite formation would be
536 prevented as documented in the presence of sulphide when FeS_x are formed (Roden and Edmonds,
537 1997). Accordingly, in our experiments, addition of sulphide to the vivianite containing sludge
538 caused a relatively quick (4 h) and significant P release.

539 Vivianite is very efficient in removing P from solution due to a very low solubility ($pK_{sp} \approx 36$, Al-
540 Borno and Tomson, 1994). Fe(II) dosing for o-P removal in oxygen free conditions resulted in
541 vivianite formation (Ghassemi, Recht 1971). The same researchers demonstrated that, in pure
542 water, stoichiometry of o-P removal was more efficient with Fe(II) compared to Fe(III), resulting
543 in lower residual o-P concentrations at optimum pH, and Fe(II) showed an optimum pH for o-P
544 removal (pH=8) closer to common sewage. On the other hand, faster kinetics of Fe(III)P
545 formation, faster settling of the formed Fe(III)P, a broader pH range for o-P removal and better
546 COD flocculation properties were found for Fe(III) (Ghassemi and Recht, 1971; Gregory and
547 O'Melia, 1989). In oxygen free freshwater (O'Connell et al., 2015; Rothe et al., 2014) and even in
548 marine sediments (Jilbert and Slomp, 2013), in anoxic soils (Nanzyo et al., 2013; Peretyazhko and
549 Sposito, 2005) and in septic tanks (Azam and Finneran, 2014) vivianite received attention as it
550 plays an important role in P retention (see recent review by Rothe et al., 2016). For the formation

551 of spherical vivianite in sediments a model has been suggested based on the presence of polymeric
552 gel structures (Zelibor et al., 1988). At least one of the crystals we found in Nieuwveer (Figure
553 2B) resembles the crystals produced by Zelibor et al., 1988, indicating that the mechanism of
554 vivianite formation could be similar in sediments and in biological STPs.

555 Similar to Frossard et al., 1997, with SEM-EDX we found larger crystals (up to 150 μm in
556 diameter) with a Fe:P ratio close to the one of vivianite in digested sludge. Such large crystals
557 were not found before digestion. The growth of the vivianite particles during digestion may be the
558 result of the additional SRT of several weeks under constantly anaerobic conditions. Ostwaldt
559 ripening, particle aggregation or crystal growth at elevated temperature in the digester may have
560 caused the growth of vivianite particles/crystals. However, vivianite showed relatively slow
561 crystal growth rates in pure solutions with higher vivianite supersaturations than observed in our
562 samples (Madsen and Hansen, 2014) and vivianite is not stable in the presence of sulphide
563 (Nriagu, 1972). Moreover, various inhibitors of Ostwald ripening, like DOC, are present during
564 the digestion process. The apparent growth of vivianite particles during the digestion process is
565 not yet fully understood.

566 XRD could not detect crystalline FeS_x in any of the samples analysed. Whereas Mössbauer
567 spectroscopy revealed that pyrite contributed significantly to the solid Fe pool and even was
568 present in the surplus sludge (9–33 % of the total Fe). The pyrite in these solids could originate
569 from the sewer system or they were formed during the treatment process (Ingvorsen et al., 2003;
570 Nielsen et al., 2005; van den Brand et al., 2015). Oxidation of FeS_x in STPs is on a time scale of
571 hours (Gutierrez et al., 2010; Ingvorsen et al., 2003; Nielsen et al., 2005), it could occur in aerated
572 zones of the STPs. However, if located in the core of the sludge flocs, FeS_x might, similar to
573 vivianite, pass aerated zone without being oxidized.

574 Quantification of P bound in FeP was performed by various approaches (Table 4). Vivianite
575 bound P contributed in Leeuwarden about 10 % before digestion and around 30 % after digestion
576 to the total solid P, according to Mössbauer spectroscopy. The quantifications using XRD
577 suggested, P in struvite contributes before digestion around 43 % and after digestion about 35 %
578 of the total P. This decrease can be explained by the external input of Fe in the digester. The
579 dissolved P concentrations are usually quite high in anaerobic digesters due to organic matter
580 degradation and, in EBPR plants, due to the release of polyphosphates from phosphate
581 accumulating organisms. Thus, vivianite formation is not limited by the supply of P. The Fe from
582 the external sludge will partly react with P to form vivianite, Fe dosing to anaerobic digesters is
583 also a measure to prevent struvite scaling as vivianite is preferably formed (Mamais et al., 1994).
584 Some of the added Fe could react with sulphide to form FeS_x . Further P could be bound in
585 biomass (phosphate accumulating organisms, cell material and debris) or in amorphous
586 compounds associated with metals like Al, Mg or Ca. To be able to identify and quantify these P
587 species would require the application of techniques like ^{31}P -NMR, sequential extraction or X-ray
588 absorption spectroscopy (e.g. Frossard et al., 1994; Wu et al., 2015). If, however, sufficient Fe(II)
589 is available, vivianite is expected to be the dominant inorganic solid P compound in digesters.
590 This would make a recovery technology targeting vivianite vastly more attractive. For Nieuwveer,
591 Mössbauer spectroscopy indicates a decrease in vivianite bound P during digestion. Here the Fe:P
592 increases only slightly due to external sludge input. Thus, the formation of FeS_x during anaerobic
593 digestion on expenses of vivianite causes a decrease in P bound to vivianite.

594 XRD might not be able to detect small particles of vivianite and amorphous FeP which Mössbauer
595 spectroscopy does detect. We consider XRD as a semi-quantitative method. In contrast to our
596 expectations, XRD did not underestimate the vivianite bound P and results of Mössbauer

597 spectroscopy were very similar (Table 4). This apparent match supports the assumption that the
598 Fe(II) fraction in Nieuwveer, that Mössbauer spectroscopy could not clearly assign to vivianite, is
599 actually vivianite. However, also the XRD results in Nieuwveer bear some uncertainty due to the
600 presence of a peak that could not be assigned. Maximum quantities of P bound in FeP, AlP and
601 MgP were estimated using the elemental composition of the TS. It was assumed that all Fe, Al and
602 Mg is bound to P and thus other fractions of these elements were neglected. However, the
603 elemental composition was, at least for the Fe, able to give good estimates on P bound to Fe.
604 Sulphide was added to sample to extract P bound to Fe (Kato et al., 2006). In Leeuwarden, the
605 sulphide extractable P fractions in digested sludge and in surplus sludge from Line 1 matched very
606 well with P in vivianite obtained from Mössbauer spectroscopy. In Nieuwveer, the release of P
607 from digested sludge in response to sulphide addition was much lower (31 %) compared to the P
608 bound in vivianite (about 50 %). However, also the molar Fe:P was about 20 % lower in the
609 sludge that was used for sulphide extraction. Translating the P release efficiency of sulphide to the
610 sludge with the 20 % higher Fe:P ratio, we would expect a P release of about 40 %. Hence,
611 sulphide extraction and Mössbauer spectroscopy would match better. It seems likely that the gap
612 between sulphide extraction and the other methods is due to a difference in the sludge samples.
613 Perhaps the released P, re-precipitated with other metals. However, from potential counter ions
614 (Mg, Ca and Al), only Ca concentrations dropped noteworthy by 2 mmol L⁻¹ (net P release was 13
615 mmol L⁻¹). Or else vivianite particles were present in Nieuwveer in another form (see Mössbauer
616 results) then the ones in Leeuwarden (e.g. more crystalline, enclosed by other minerals/organic)
617 that made vivianite less reactive/unreactive to sulphide exposure. Overall, all methods gave good
618 estimates for P bound to Fe and for P bound in vivianite. The elemental composition is the easiest
619 method but gives the less accurate result. Sulphide extractions is relatively simple, here P is

620 released from all Fe compounds without determining the type of FeP present. XRD is a popular
621 and common method. It allows the quantification of crystalline FeP only. In our case all Fe bound
622 P was vivianite, hence the quantification worked well. In sludge with amorphous FeP or dispersed
623 vivianite, XRD will not be able to quantify P bound to Fe. Mössbauer spectroscopy is, however,
624 able to detect amorphous and crystalline Fe compounds very accurately. In Nieuwveer, about 1/3
625 of the Fe(II) that was assigned to vivianite could also be another Fe(II) phase. Preparation of
626 appropriate standards may help to identify this Fe(II) using Mössbauer spectroscopy in future. In
627 general, Mössbauer gives very accurate qualitative/quantitative results but it should be used in
628 combination with other complementary methods like XRD.

629 **5 Conclusion**

630 Mössbauer spectroscopy indicated that vivianite and pyrite were the dominating solid Fe
631 compounds in the surplus and anaerobically digested sludge from two STPs applying CPR and
632 EBPR. XRD confirmed that vivianite was the major FeP in the samples. None of the sludge
633 samples contained a significant amount of Fe(III) although besides Fe(II) also Fe(III) was dosed.
634 Likely, this is related to fast iron reduction processes and slow vivianite oxidation rates. Studying
635 Fe chemistry, helped to identify measures on how sewage treatment can be improved. In
636 Leeuwarden, Fe dosing, to prevent sulphide emissions, can be reduced. In Nieuwveer, improving
637 the aeration to form Fe(III) would improve COD removal in the A-stage. To assess the role of
638 vivianite and the potential of a P recovery technology targeting on FeP, further STPs with
639 different treatment designs (higher Fe dosing and particularly higher Fe(III) dosing) should be
640 analysed as well. If vivianite is a general iron precipitant in STPs it could offer new routes for P
641 recovery.

642 **Acknowledgements**

643 This work was performed in the TTIW-cooperation framework of Wetsus, European Centre Of
644 Excellence For Sustainable Water Technology (www.wetsus.nl). Wetsus is funded by the Dutch
645 Ministry of Economic Affairs, the European Union Regional Development Fund, the Province of
646 Fryslân, the City of Leeuwarden and the EZ/Kompas program of the “Samenwerkingsverband
647 Noord-Nederland”. We thank the participants of the research theme “Phosphate Recovery” for
648 their financial support and helpful discussions. We acknowledge the great support by employees
649 of Waterschap Brabantse Delta, Wetterskip Fryslan and from the two STPs.

650 **6 References**

- 651 Al-Borno, A., Tomson, M.B., 1994. The temperature dependence of the solubility product
652 constant of vivianite. *Geochimica et Cosmochimica Acta* 58 (24), 5373–5378.
- 653 APHA, AWWA, WEF, 1998. Standard methods for the examination of water and wastewater,
654 20th ed. 1998 ed. American Public Health Association, Washington, DC.
- 655 Azam, H.M., Finneran, K.T., 2014. Fe(III) reduction-mediated phosphate removal as vivianite
656 ($\text{Fe}_3(\text{PO}_4)_2 \cdot 8\text{H}_2\text{O}$) in septic system wastewater. *Chemosphere* 97, 1–9.
- 657 Biber, M.V., dos Santos Afonso, M., Stumm, W., 1994. The coordination chemistry of
658 weathering: IV. Inhibition of the dissolution of oxide minerals. *Geochimica et Cosmochimica*
659 *Acta* 58 (9), 1999–2010.
- 660 Böhnke, B., 1977. Das Adsorptions-Belebungsverfahren. *Korrespondenz Abwasser* 24.
- 661 Böhnke, B., Diering, B., Zuckut, S.W., 1997. Cost-effective wastewater treatment process for
662 removal of organics and nutrients. *Water Eng. Manag.* 144 (7), 18–21.

- 663 Buffle, J., 1990. Complexation reactions in aquatic systems: an analytical approach. Ellis
664 Horwood series in analytical chemistry. Ellis Horwood.
- 665 Carliell-Marquet, C., Oikonomidis, I., Wheatley, A., Smith, J., 2009. Inorganic profiles of
666 chemical phosphorus removal sludge. *Proceedings of the ICE - Water Management* 163 (2),
667 65–77.
- 668 Carpenter, S.R., 2008. Phosphorus control is critical to mitigating eutrophication. *Pro. Natl.*
669 *Acad.Sci. USA* 105, 11039–11040.
- 670 Carpenter, S.R., Bennett, E.M., 2011. Reconsideration of the planetary boundary for phosphorus.
671 *Environ. Res. Lett.* 6 (1), 14009.
- 672 Čermáková, Z., Švarcová, S., Hradilová, J., Bezdička, P., Lančok, A., Vašutová, V., Blažek, J.,
673 Hradil, D., 2015. Temperature-related degradation and colour changes of historic paintings
674 containing vivianite. *Spectrochimica Acta Part A: Molecular and Biomolecular Spectroscopy*
675 140, 101–110.
- 676 Cheng, X., Chen, B., Cui, Y., Sun, D., Wang, X., 2015. Iron(III) reduction-induced phosphate
677 precipitation during anaerobic digestion of waste activated sludge. *Separation and Purification*
678 *Technology* 143, 6–11.
- 679 Childers, D.L., Corman, J., Edwards, M., Else, J.J., 2011. Sustainability challenges of phosphorus
680 and food: solutions from closing the human phosphorus cycle. *Bioscience* 61 (117-124).
- 681 Cline, J.D., 1969. Spectrophotometric determination of hydrogensulfide in natural waters. *Limnol.*
682 *Oceangr.* 14, 454–458.
- 683 Davison, W., 1991. The solubility of iron sulphides in synthetic and natural waters at ambient
684 temperature. *Aquatic Science* 53 (4), 309–329.

- 685 De Graaff, M., Roest, D., Brand Van Den, T., Zandvoort, M., Duin, O., van Loosdrecht, M., 2015.
686 Characterisation of high loaded wastewater treatment processes (A-stage) to increase energy
687 production from wastewater: performance and design guidelines. *Water research* (accepted).
- 688 De Ridder, M., De Jong, S., Polchar, J., Lingemann, S., 2012. Risks and opportunities in the
689 global phosphate rock market: Robust strategies in times of uncertainty. Rapport / Centre for
690 Strategic Studies no. 17 | 12 | 12. The Hague Centre for Strategic Studies, Den Haag.
- 691 Dyar, M.D., Jawin, E.R., Breves, E., Marchand, G., Nelms, M., Lane, M.D., Mertzman, S.A.,
692 Bish, D.L., Bishop, J.L., 2014. Mossbauer parameters of iron in phosphate minerals:
693 Implications for interpretation of martian data. *American Mineralogist* 99 (5-6), 914–942.
- 694 Eeckhout, S.G., Grave, E. de, Vochten, R., Blaton, N.M., 1999. Mössbauer effect study of
695 anapaite, $\text{Ca}_2\text{Fe}^{2+}(\text{PO}_4)_2 \cdot 4\text{H}_2\text{O}$, and of its oxidation products. *Physics and Chemistry*
696 *of Minerals* 26 (6), 506–512.
- 697 El Samrani, A.G., Lartiges, B.S., Montarges-Pelletier, E., Kazpard, V., Barres, O., Ghanbaja, J.,
698 2004. Clarification of municipal sewage with ferric chloride: The nature of coagulant species.
699 *Water research* 38, 756–768.
- 700 Frossard, E., Bauer, J.P., Lothe, F., 1997. Evidence of vivianite in FeSO_4 -flocculated sludges.
701 *Water research* 31 (10), 2449–2454.
- 702 Frossard, E., Tekely, P., Grimal, J.Y., 1994. Characterization of phosphate species in urban sewage
703 sludges by high-resolution solid-state ^{31}P NMR. *Eur J Soil Science* 45, 403–408.
- 704 Fulazzaky, M.A., Salim, N., Abdullah, N.H., Yusoff, A., Paul, E., 2014. Precipitation of iron-
705 hydroxy-phosphate of added ferric iron from domestic wastewater by an alternating aerobic–
706 anoxic process. *Chemical Engineering Journal* 253, 291–297.

- 707 Gaffney, J.W., White, K.N., Boulton, S., 2008. Oxidation State and Size of Fe Controlled by
708 Organic Matter in Natural Waters. *Environ. Sci. Technol.* 42 (10), 3575–3581.
- 709 Geraarts, B., Koetse, E., Loeffen, P., Reitsma, B., Gaillard, A., 2007. Fosfaatterugwinning uit
710 ijzerarm slib van rioolwaterzuiveringsinrichtingen. STOWA, 83 pp.
711 http://www.stowa.nl/Upload/publicaties2/mID\4924_cID\3914_74684671_STOWA 2007
712 31.pdf.
- 713 Ghassemi, M., Recht, H.L., 1971. Phosphate Precipitation with Ferrous Iron. *Water Pollution*
714 *Control Research Series*, 64 pp.
- 715 Golterman, H.L., 2001. Phosphate release from anoxic sediments or ‘What did Mortimer really
716 write?’. *Hydrobiologia* 450 (1/3), 99–106.
- 717 Gonser, U., Grant, R.W., 1976. Determination of spin directions and electric fields gradient axes
718 in vivianite by polarized recoil free γ -Rays. *Phys. Stat. Sol.* 21 (331).
- 719 Gregory, J., O'Melia, C.R., 1989. Fundamentals of flocculation. *Critical Reviews in*
720 *Environmental Control* 19 (3), 185–230.
- 721 Gutierrez, O., Park, D., Sharma, K.R., Yuan, Z., 2010. Iron salts dosage for sulfide control in
722 sewers induces chemical phosphorus removal during wastewater treatment. *Water research* 44
723 (11), 3467–3475.
- 724 Harker, S.J., Pollard, R.J., 1993. A study of magnetite at 4.2 K and subject to strong applied
725 magnetic fields. *Nuclear Instruments and Methods in Physics Research Section B: Beam*
726 *Interactions with Materials and Atoms* 76 (1-4), 61–63.
- 727 Higgins, M., Murthy, S., 2006. Understanding factors affecting polymer demand for thickening
728 and dewatering. Water Environment Research Foundation; IWA Publishing, Alexandria, Va,
729 London.

- 730 Hsu, P.H., 1976. Comparison of iron(III) and aluminum in precipitation of phosphate from
731 solution. *Water research* 10 (10), 903–907.
- 732 Hvitved-Jacobsen, T., Vollertsen, J., Nielsen, A.H., 2013. *Sewer processes: Microbial and*
733 *chemical process engineering of sewer networks*, 2nd ed. ed. CRC Press, Boca Raton.
- 734 Ingvorsen, K., Nielsen, M.Y., Joulain, C., 2003. Kinetics of bacterial sulfate reduction in an
735 activated sludge plant. *Microb Ecol* 46, 129–137.
- 736 Jackson, A., Gaffney, J.W., Boulton, S., 2012. Subsurface interactions of Fe(II) with humic acid or
737 landfill leachate do not control subsequent iron(III) (hydr)oxide production at the surface.
738 *Environ. Sci. Technol.* 46 (14), 7543–7550.
- 739 Jetten, M., Horn, S., van Loosdrecht, M.C.M., 1997. Towards a more sustainable municipal
740 wastewater treatment system. *Water Science & Technology* 35 (9), 171–180.
- 741 Jilbert, T., Slomp, C.P., 2013. Iron and manganese shuttles control the formation of authigenic
742 phosphorus minerals in the euxinic basins of the Baltic Sea. *Geochimica et Cosmochimica*
743 *Acta* 107, 155–169.
- 744 Kappler, A., Benz, M., Schink, B., Brune, A., 2004. Electron shuttling via humic acids in
745 microbial iron(III) reduction in a freshwater sediment. *FEMS Microbiology Ecology* 47 (1),
746 85–92.
- 747 Kato, F., Kitakoji, H., Oshita, K., Takaoka, M., Takeda, N., Matsumoto, T., 2006. Extraction
748 efficiency of phosphate from pre-coagulated sludge with NaHS. *Water Science & Technology*
749 54 (5), 119.
- 750 Klencsár, Z., 1997. Mössbauer spectrum analysis by Evolution Algorithm. *Nuclear Instruments*
751 *and Methods in Physics Research Section B: Beam Interactions with Materials and Atoms* 129
752 (4), 527–533.

- 753 Kraal, P., Slomp, C.P., Forster, A., Kuypers, M., Sluijs, A., 2009. Pyrite oxidation during sample
754 storage determines phosphorus fractionation in carbonate-poor anoxic sediments. *Geochimica
755 et Cosmochimica Acta* 73, 3277–3290.
- 756 Kracht, O., Gresch, M., Gujer, W., 2007. A Stable Isotope Approach for the Quantification of
757 Sewer Infiltration. *Environ. Sci. Technol.* 41 (16), 5839–5845.
- 758 Leavens, P.B. (Ed.), 1972. Oxidation of vivianite in New Jersey Cretaceous greensands.
- 759 Li, J., 2005. Effects of Fe(III) on floc characteristics of activated sludge. *J. Chem. Technol.
760 Biotechnol.* 80 (3), 313–319.
- 761 Luedecke, C., Hermanowicz, S.W., Jenkins, D., 1989. Precipitation of ferric phosphate in
762 activated-sludge - A chemical model and its verification. *Water Science & Technology* 21 (4-
763 5), 325–337.
- 764 Macdonald, G.K., Bennett, E.M., Potter, P.A., Ramankutty, N., 2011. Agronomic phosphorus
765 imbalances across the world's croplands 108 (7), 3086–3091.
- 766 Madsen, H., Hansen, H., 2014. Kinetics of crystal growth of vivianite, $\text{Fe}_3(\text{PO}_4)_2 \times 8\text{H}_2\text{O}$, from
767 solution at 25, 35 and 45 °C. *Journal of Crystal Growth* (401), 82–86.
- 768 Mamais, D., Pitt, P.A., Cheng, Y.W., Loiacono, J., Jenkins, D., 1994. Determination of ferric
769 chloride dose to control struvite precipitation in anaerobic sludge digesters. *Water Environ Res*
770 66 (7), 912–918.
- 771 McKeague, J.A., 1967. An evaluation of 0.1 M pyrophosphate and pyrophosphate-dithionite in
772 comparison with oxalate as extractants of accumulation products in podzols and some other
773 soils. *Can. J. Soil. Sci.* 47 (2), 95-&.

- 774 Miot, J., Benzerara, K., Morin, G., Bernard, S., Beyssac, O., Larquet, E., Kappler, A., Guyot, F.,
775 2009. Transformation of vivianite by anaerobic nitrate-reducing iron-oxidizing bacteria.
776 *Geobiology* 7 (3), 373–384.
- 777 Mullet, M., Boursiquot, S., Abdelmoula, M., Génin, J.M., Ehrhardt, J.J., 2002. Surface chemistry
778 and structural properties of mackinawite prepared by reaction of sulfide ions with metallic
779 iron. *Geochimica et Cosmochimica Acta* 66 (5), 829–836.
- 780 Murad, E., Cashion, J., 2004. Mössbauer Spectroscopy of Environmental Materials and Their
781 Industrial Utilization. Springer US, Boston, MA.
- 782 Nanzyo, M., Onodera, H., Hasegawa, E., Ito, K., Kanno, H., 2013. Formation and Dissolution of
783 Vivianite in Paddy Field Soil. *Soil Science Society of America Journal* 77 (4), 1452.
- 784 Nielsen, A.H., Lens, P., Vollertsen, J., Hvitved-Jacobsen, T., 2005. Sulfide–iron interactions in
785 domestic wastewater from a gravity sewer. *Water research* 39 (12), 2747–2755.
- 786 Nielsen, J.L., Nielsen, P.H., 1998. Microbial Nitrate-Dependent Oxidation of Ferrous Iron in
787 Activated Sludge. *Environ. Sci. Technol.* 32, 3556–3561.
- 788 Nielsen, P., 1996. The significance of microbial Fe(III) reduction in the activated sludge process.
789 *Water Science & Technology* 34 (5-6), 129–136.
- 790 Nriagu, J.O., 1972. Stability of vivianite and ion-pair formation in the system $Fe_3(PO_4)_2$ -
791 H_3PO_4 - H_2O . *Geochimica et Cosmochimica Acta* 36 (4), 459–470.
- 792 O'Connell, D.W., Jensen, M.M., Jakobsen, R., Thamdrup, B., Andersen, T.J., Kovacs, A., Hansen,
793 H., 2015. Vivianite formation and its role in phosphorus retention in Lake Ørn, Denmark.
794 *Chemical Geology* 409, 42–53.
- 795 Oikonomidis, I., Burrows, L.J., Carliell-Marquet, C., 2010. Mode of action of ferric and ferrous
796 iron salts in activated sludge. *J. Chem. Technol. Biotechnol.* 85 (8), 1067–1076.

- 797 Paul, E., Laval, M.L., Sperandio, M., 2001. Excess sludge production and costs due to phosphorus
798 removal. *Environmental technology* 22, 1363–1371.
- 799 Peretyazhko, T., Sposito, G., 2005. Iron(III) reduction and phosphorous solubilization in humid
800 tropical forest soils. *Geochimica et Cosmochimica Acta* 69 (14), 3643–3652.
- 801 Poffet, M.S., 2007. Thermal runaway of the dried sewage sludge in the storage tanks: from
802 molecular origins to technical measures of smouldering fire prevention. Dissertation thesis.
- 803 Rasmussen, H., Nielsen, P., 1996. Iron reduction in activated sludge measured with different
804 extraction techniques. *Water research* 30 (3), 551–558.
- 805 Recht, H.L., Ghassemi, M., 1970. Kinetics and mechanism of precipitation and nature of the
806 precipitate obtained in phosphate removal from wastewater using aluminum(III) and iron(III)
807 salts. *Water Pollution Control Research Series*. U.S. Dept. of the Interior, FWQA.
- 808 Roden, E.E., Edmonds, J.W., 1997. Phosphate mobilization in iron-rich anaerobic sediments:
809 Microbial Fe(III) oxide reduction versus iron-sulfide formation. *Archiv für Hydrobiologie* 139
810 (3), 347–378.
- 811 Roldan, R., Barron, V., Torrent, J., 2002. Experimental alteration of vivianite to lepidocrocite in a
812 calcareous medium. *clay miner* 37 (4), 709–718.
- 813 Rothe, M., Frederichs, T., Eder, M., Kleeberg, A., Hupfer, M., 2014. Evidence for vivianite
814 formation and its contribution to long-term phosphorus retention in a recent lake sediment: A
815 novel analytical approach. *Biogeosciences* 11 (18), 5169–5180.
- 816 Rothe, M., Kleeberg, A., Hupfer, M., 2016. The occurrence, identification and environmental
817 relevance of vivianite in waterlogged soils and aquatic sediments. *Earth-Science Reviews* 158,
818 51–64.

- 819 Scholz, R.W., Wellmer, F.W., 2016. Comment on: "Recent revisions of phosphate rock reserves
820 and resources: a critique" by Edixhoven et al. (2014) – clarifying comments and thoughts on
821 key conceptions, conclusions and interpretation to allow for sustainable action. *Earth Syst.*
822 *Dynam.* 7 (1), 103–117.
- 823 Seitz, M.A., Riedner, R.J., Malhotra, S.K., Kipp, R.J., 1973. Iron-phosphate compound
824 identification in sewage sludge residue. *Environ. Sci. Technol.* 7 (4), 354–357.
- 825 Siegrist, H., Salzgeber, D., Eugster, J., Joss, A., 2008. Anammox brings WWTP closer to energy
826 autarky due to increased biogas production and reduced aeration energy for N-removal. *Water*
827 *Science & Technology* 57 (3), 383–388.
- 828 Singer, P.C., 1972. Anaerobic control of phosphate by ferrous iron: Anaerobic control of
829 phosphate by ferrous iron. *Journal Water Pollution Control Federation* 44 (4), 663-&.
- 830 Sklute, E.C., Jensen, H.B., Rogers, A.D., Reeder, R.J., 2015. Morphological, structural, and
831 spectral characteristics of amorphous iron sulfates. *J. Geophys. Res. Planets* 120 (4), 809–830.
- 832 Smith, S., Takacs, I., Murthy, S., Daigger, G.T., Szabo, A., 2008. Phosphate complexation model
833 and its implications for chemical phosphorus removal. *Water Environ Res* 80 (5), 428–438.
- 834 Stucki, J.W., 2013. *Iron in soils and clay minerals*. Springer, [Place of publication not identified].
- 835 Szabó, A., Takács, I., Murthy, S., Daigger, G.T., Licskó, I., Smith, S., 2008. Significance of
836 Design and Operational Variables in Chemical Phosphorus Removal. *Water Environ Res* 80
837 (5), 407–416.
- 838 Takács, I., Murthy, S., Smith, S., McGrath, M., 2006. Chemical phosphorus removal to extremely
839 low levels: experience of two plants in the Washington, DC area. *Water Science &*
840 *Technology* 53 (12), 21.

- 841 Tchobanoglous, G., Burton, F.L., Stensel, H.D., 2013. Wastewater engineering: Treatment and
842 reuse, 5th ed. ed. McGraw-Hill Higher Education; McGraw-Hill [distributor], New York,
843 London.
- 844 Thomas, A.E., 1965. Phosphat-Elimination in der Belebtschlammanlage von Männedorf und
845 Phosphat-Fixation in See- und Klärschlamm. Vierteljahrsschr. Naturforsch. Ges. Zürich 110,
846 419–434.
- 847 van den Brand, T. P. H., Roest, K., Chen, G. H., Brdjanovic, D., van Loosdrecht, M. C. M., 2015.
848 Occurrence and activity of sulphate reducing bacteria in aerobic activated sludge systems.
849 World J Microbiol Biotechnol 31 (3), 507–516.
- 850 van den Kerk, A.J., 2005. Vervolgonderzoek rioolvreemd water. STOWA, Utrecht.
- 851 van Dijk, K.C., Lesschen, J.P., Oenema, O., 2016. Phosphorus flows and balances of the
852 European Union Member States. Science of The Total Environment 542, 1078–1093.
- 853 van Hullebusch, E.D., Utomo, S., Zandvoort, M., Lens, P., 2005. Comparison of three sequential
854 extraction procedures to describe. Talanta 65, 549–558.
- 855 Verschoor, M.J., Molot, A.M., 2013. A comparison of three colorimetric methods of ferrous and
856 total reactive iron measurement in freshwaters (11), 113–125.
- 857 Viollier, E., Inglett, P.W., Hunter, K., Roychoudhury, A.N., van Cappellen, P., 2000. The
858 ferrozine method revisited: Fe(II)/Fe(III) determination in natural waters. Applied
859 Geochemistry 15 (6), 785–790.
- 860 Walan, P., Davidsson, S., Johansson, S., Höök, M., 2014. Phosphate rock production and
861 depletion: Regional disaggregated modeling and global implications. Resources, Conservation
862 and Recycling 93, 178–187.

- 863 WEF, 2011. Nutrient removal. WEF manual of practice no. 34. McGraw-Hill; WEF Press, New
864 York, Alexandria, Va.
- 865 Wilfert, P., Suresh Kumar, P., Korving, L., Witkamp, G.J., van Loosdrecht, M.C.M., 2015. The
866 relevance of phosphorus and iron chemistry to the recovery of phosphorus from wastewater: a
867 review. *Environ. Sci. Technol.*
- 868 Wolf, A.M., Moore, P.A., Kleinman, P., Sullivan, D.M., 2009. Water-Extractable Phosphorus in
869 Animal Manure and Biosolids, in: *Methods for Phosphorus Analysis for Soils, Sediments,
870 Residuals, and Waters*, pp. 76–80.
- 871 Wu, H., Ikeda-Ohno, A., Wang, Y., Waite, T.D., 2015. Iron and phosphorus speciation in Fe-
872 conditioned membrane bioreactor activated sludge. *Water research* 76, 213–226.
- 873 Yoshida, Y., Langouche, G. (Eds.), 2013. *Mossbauer spectroscopy: Tutorial book*. Springer,
874 Berlin, New York.
- 875 Zelibor, J.L., Senftle, F.E., Reinhardt, J.L., 1988. A proposed mechanism for the formation of
876 spherical vivianite crystal aggregates in sediments. *Sedimentary Geology* 59 (1-2), 125–142.
- 877 Zhang, X., 2012. Factors Influencing Iron Reduction–Induced Phosphorus Precipitation.
878 *Environmental Engineering Science* 29 (6), 511–519.

879 7 Supporting information

ACCEPTED MANUSCRIPT

880 Table A. 1: Measured parameters in the STP Leeuwarden. The reported values are the mean and the standard deviation of the three measurement
 881 campaigns between December 2013 and February 2014. In each campaign all measurements were made in triplicates. The Effluent from line 2
 882 was only measured once.

LWD	T (°C)	pH	ORP (mV)	TS (g/kg)	VS (g/kg)	TA (mEq/L)	Fe(II) (mg/L)	Fe(III) (mg/L)	Total Dissolved Fe-Ferrozine (mg/L)	Total Dissolved Fe-ICP (mg/L)	Total Fe (mg/kg)	Total Solid Fe (mg/g TS)	o-P (mg P/L)	Total Dissolved P (mg/L)	Total P (mg/kg)	Total Solid P (mg/g TS)	S-SO4 (mg S/L)	Total Dissolved S (mg/L)	Total S (mg/kg)	Total Solid S (mg/g TS)
Influent	11.6 (4.6)	7.9 (0.1)	-195 (61)	1.2 (0.2)	0.4 (0.1)	10.4 (4.4)	0	0.3	0.3 (0)	0.2 (0.1)	1.7 (0.4)	1.2 (0.2)	4.5 (2.8)	5.3 (3.1)	7.5 (3.8)	2.1 (1)	9.6 (1.9)	9.4 (3.1)	18.2 (8.3)	7.5 (7.6)
Effluent line 1	11.2 (1.6)	7.6 (0.2)	62 (63)	0.7 (0.2)	0.1 (0.0)	6.9 (0.5)	0	0.1	0.1 (0.1)	0.1 (0.0)	0.3 (0.1)	0.1 (0.1)	0.4 (0.3)	0.5 (0.4)	0.9 (0.4)	0.5 (0.4)	11 (1.2)	10.5 (1.2)	15.7 (5.5)	8.4 (10.2)
Effluent line 2	12.2	7.8	45	0.9	0.1 (n.d.)	5.6 (n.d.)	0	0.1	0.1	0.1	0.5	0.4	0.2	0.3	0.4	0.2	12.4	13	13.6	0.7
Before Fe dosing line 2	11.4 (4.6)	7.4 (0.1)	-156 (35)	4.2 (0.1)	3 (0.2)	9.1 (1.5)	0.1	0.6	0.7 (0.3)	0.7 (0.3)	52.5 (9.5)	12.2 (2.0)	10.1 (9.9)	11.2 (10.4)	109.8 (16.9)	23.4 (1.4)	11 (1.8)	10.1 (2.6)	38 (1.8)	6.6 (0.6)
After Fe dosing line 2	11.7 (4.5)	7.3 (0.0)	-18 (40)	4.7 (0.4)	3.2 (0.3)	7.6 (0.9)	0.1	0.5	0.6 (0.3)	0.5 (0.3)	59.1 (16.3)	12.7 (3.7)	1.6 (0.6)	2 (0.8)	119.8 (19.9)	25.2 (2.2)	11.3 (1)	10.4 (2.5)	41.8 (10.1)	6.7 (1.8)
Surplus sludge line 1	12.3 (2.7)	7.4 (0.1)	-42 (75)	69 (0.7)	4.9 (0.7)	8.9 (0.7)	0.1	0.5	0.6 (0.1)	0.5 (0.1)	106.4 (25.2)	15.3 (2.7)	2.7 (1.2)	3.4 (1.4)	188.9 (9.1)	27.1 (2.2)	11.4 (1.2)	10.5 (2.1)	53.9 (5.1)	6.4 (0.4)
Surplus sludge line 2	12.4 (3.7)	7.3 (0.0)	-90 (8)	69 (0.3)	4.9 (0.1)	9.5 (0.7)	0.6	0.6	1.1 (0.3)	1.2 (0.4)	96.8 (37.8)	13.8 (4.9)	4.3 (0.4)	5.6 (0.0)	192 (5.7)	26.9 (0.6)	11.2 (1.6)	11 (3.5)	58.3 (8.3)	6.9 (0.4)
Digested sludge	29.3 (0.2)	7.4 (0.1)	-380 (27)	45.6 (0.7)	28.4 (0.8)	157.8*/211.7** (11.9/30.8)	0.6	1.6	2.1 (0.2)	1.7 (0.4)	1849.7 (92.3)	40.5 (1.9)	169.6 (22.4)	179.3 (33.6)	1970.6 (149.1)	39.4 (3.3)	5.1 (2.4)	7.1 (1.8)	418.5 (21.6)	9 (0.4)

*Supernatant after centrifugation

** Raw sludge

LWD	Total Dissolved Al (mg/L)	Total Al (mg/kg)	Total Solid Al (mg/g TS)	Total Dissolved Mg (mg/L)	Total Mg (mg/kg)	Total Solid Mg (mg/g TS)	Total Dissolved Ca (mg/L)	Total Ca (mg/kg)	Total Solid Ca (mg/g TS)	Total Dissolved K (mg/L)	Total K (mg/kg)	Total Solid K (mg/g TS)	Total Dissolved Na (mg/L)	Total Na (mg/kg)	Total Solid Na (mg/g TS)
Influent	<0.1	<1.25	-	12.3 (0.7)	13.9 (2.4)	1.7 (2.4)	64.1 (12.3)	75 (9.7)	10.6 (9.3)	20.6 (9.8)	25.8 (14.6)	4.5 (4.1)	178.6 (43.8)	213.6 (14.6)	34.1 (29.9)
Effluent line 1	<0.05	<1.25	-	10.3 (1.6)	11 (1.6)	1.1 (0.6)	58.4 (11.2)	64 (9)	8.8 (4.9)	13.5 (2)	15.4 (2.8)	2.2 (2.9)	164.3 (48.2)	173.5 (45.7)	14 (7.3)
Effluent line 2	<0.05	<1.25	-	12.9	13.2	0.3	72.4	75.2	3.3	13.2	17.4	4.8	194.5	201	7.7
Before Fe dosing line 2	<0.2	21.2 (1.2)	5 (0.4)	13.6 (1.5)	34.4 (1.8)	4.9 (0.1)	59.8 (15.9)	151.3 (17.6)	21.7 (7.4)	21.1 (7.4)	54.1 (2.1)	7 (1.2)	168.1 (61.7)	181.8 (61.9)	3.4 (1.1)
After Fe dosing line 2	<0.1	23 (1.5)	5 (0.6)	11.7 (1.6)	36.9 (3.7)	5.4 (0.6)	61 (12.2)	158.2 (22.2)	20.7 (3.9)	16.2 (1.9)	57.64 (2.7)	36.8 (49.1)	154.3 (43.6)	168.2 (46.6)	3.1 (0.8)
Surplus sludge line 1	<0.2	34.3 (7.9)	5 (0.7)	11.8 (1.5)	50.5 (2)	5.7 (0.7)	58.8 (10.8)	207.8 (11.3)	22 (3.8)	18.1 (0.3)	78.7 (5.4)	25 (27.2)	168.2 (50.4)	191.5 (43.4)	3.6 (1.3)
Surplus sludge line 2	< 0.2	34.7 (7.6)	5 (0.9)	13 (2.9)	51 (3)	5.5 (0.2)	59.8 (15.6)	205.8 (0.4)	21.3 (3.1)	19.8 (1)	76.7 (10.0)	8.3 (1.0)	163.7 (47.1)	171.8 (45.0)	1.3 (0.3)
Digested sludge	<0.5	239.8 (17.4)	5.3 (0.4)	5.4 (4.5)	370.8 (37.5)	8 (0.8)	49.9 (5.2)	1901 (183.7)	40.6 (3.5)	500.4 (29.2)	551.4 (29.0)	1.6 (0.6)	263.2 (12.2)	289.8 (49.5)	0.8 (0.8)

883

884

885

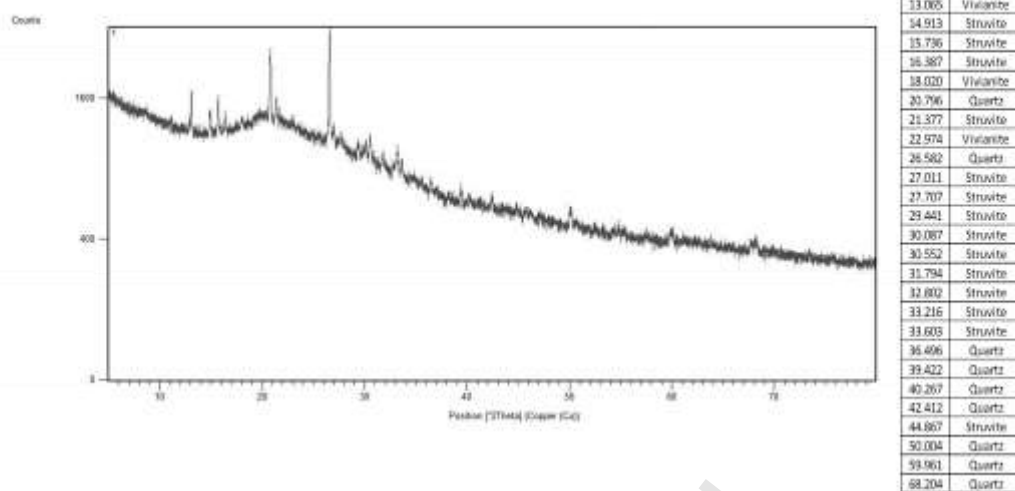
886 Table A. 2: Measured parameters in the STP Nieuwveer. Nieuwveer was only sampled once in March 2014. The reported values are the mean and
 887 standard deviation of triplicate measurements.

Nieuwveer	T (°C)	pH	ORP (mV)	TS (g/kg)	VS (g/kg)	TA (mEq/L)	Fe(II) (mg/L)	Fe(III) (mg/L)	Total Dissolved Fe-Ferrozine (mg/L)	Total Dissolved Fe-ICP (mg/L)	Total Fe (mg/kg)	Total Solid Fe (mg/g TS)	o-P (mg P L ⁻¹)	Total Dissolved P (mg/L)	Total P (mg/kg)	Total Solid P (mg/g TS)	SO4 (mg S L ⁻¹)	Total Dissolved S (mg/L)	Total S (mg/kg)	Total Solid S (mg/g TS)
Influent	9.8	7.3	10	0.4 (0.01)	0.1 (0.01)	4.6	0	0.3 (0.0)	0.3 (0.0)	0.2	0.86 (0.0)	1.4	1.6	2.0	2.9 (0.0)	2.3	10.8	10.8	11.3 (0.2)	1.4
Effluent	9.7	7	117	0.3 (0.02)	0.08 (0.0)	2.1	0.0	0.1 (0.0)	0.09 (0.0)	0.1	0.23 (0.0)	0.5	0.8	1.1	1.3 (0.0)	0.7	10.8	9.9	10.4 (0.1)	1.6
A-stage	9.4	7.1	-90	3.6 (0.1)	2.8 (0.1)	11.8	0.0	0.8 (0.1)	0.8 (0.1)	0.8	82.5 (2.1)	22.4	1.0	1.5	57.7 (0.5)	15.4	12.0	11.2	20.9 (2.1)	2.7
A-stage: Surplus sludge	10	6.8	-264	18.6 (0.1)	14.8 (0.1)	13.2	18.3 (1.1)	12.7 (0.1)	31 (1.2)	32.4	436.7 (23.6)	21.8	18.9	31.2	290.2 (15.3)	13.9	10.0	16.8	89.5 (2.6)	3.9
B-stage: Surplus sludge	9.4	7	-109	14.9 (0.3)	11.6 (0.2)	9.1	0.0	1.9 (0.0)	1.9 (0.03)	1.4	426.7 (9.4)	28.6	5.5	7.2	375 (7.1)	24.8	10.9	11.4	107.8 (3.5)	6.5
External sludge before digestion	17	6	-294	75.9 (8.1)	58.3 (5.9)	30.2	70.7 (1.2)	26.8 (26.9)	97.6 (7.8)	90.0	1747 (139)	21.8	12.9	54.8	1121.8 (82.9)	14.1	18.6	15.3	347 (21.6)	4.4
Digested sludge	27	7.7	-322	41.6 (0.1)	24.8 (0.7)	140.7	0.1 (0.0)	3.0 (0.1)	3.1 (0.1)	3.0	2389 (78.7)	57.4	70.2	73.8	1558.2 (29.2)	35.8	7.1	14.5	442.2 (8.4)	10.3

888

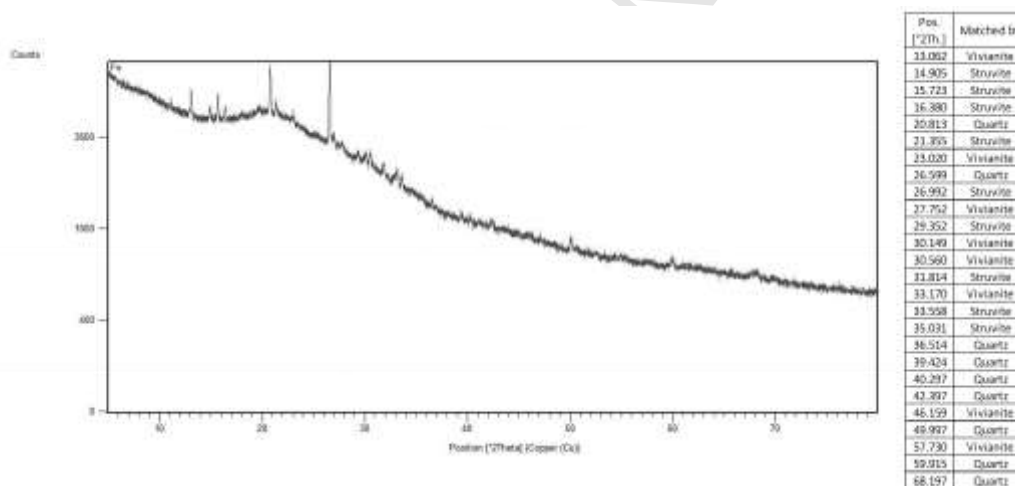
Nieuwveer	Total Dissolved Al (mg/L)	Total Al (mg/kg)	Total Solid Al (mg/g TS)	Total Dissolved Mg (mg/L)	Total Mg (mg/kg)	Total Solid Mg (mg/g TS)	Total Dissolved Ca (mg/L)	Total Ca (mg/kg)	Total Solid Ca (mg/g TS)	Total Dissolved K (mg/L)	Total K (mg/kg)	Total Solid K (mg/g TS)	Total Dissolved Na (mg/L)	Total Na (mg/kg)	Total Solid Na (mg/g TS)
Influent	<0.1	0.3 (0.0)	0.9	5.2	5.6 (0.0)	1.2	44.0	45.7 (0.1)	4.7	14.0	14.6 (0.2)	1.5	48.8	47.1 (0.2)	-
Effluent	<0.05	<0.2	-	4.5	4.7 (0.1)	0.7	37.3	37.9 (0.5)	2.2	11.2	12.9 (0.2)	5.5	43.6	42.7 (0.7)	-
A-stage	<0.5	19.4 (1.6)	5.3	4.7	<17	-	40.3	143.3 (5.2)	28.3	13.1	34.8 (0.7)	6	45.4	<83	-
A-stage: Surplus sludge	<0.2	82.2 (7.3)	4.4	10.7	39.7 (2.8)	1.6	88.5	373.3 (23.6)	15.4	34.7	69.7 (4.7)	1.9	56.7	<83	-
B-stage: Surplus sludge	<0.2	77.5 (1.1)	5.2	5.6	46 (0.9)	2.7	39.8	309.5 (10.1)	18.2	20.5	100.5 (4.9)	5.4	44.4	<83	-
External sludge before digestion	<0.5	451.5 (50.4)	5.9	34.2	137.2 (4.6)	1.4	215.5	1226.4 (40.5)	13.5	107.5	252.3 (12.4)	2	62.5	<170	-
Digested sludge	<0.5	479.9 (5.2)	11.5	12.5	170.9 (4.2)	3.8	41.8	1251.2 (13.9)	29.1	196.0	267.3 (2.5)	1.9	81.1	<160	-

889



890

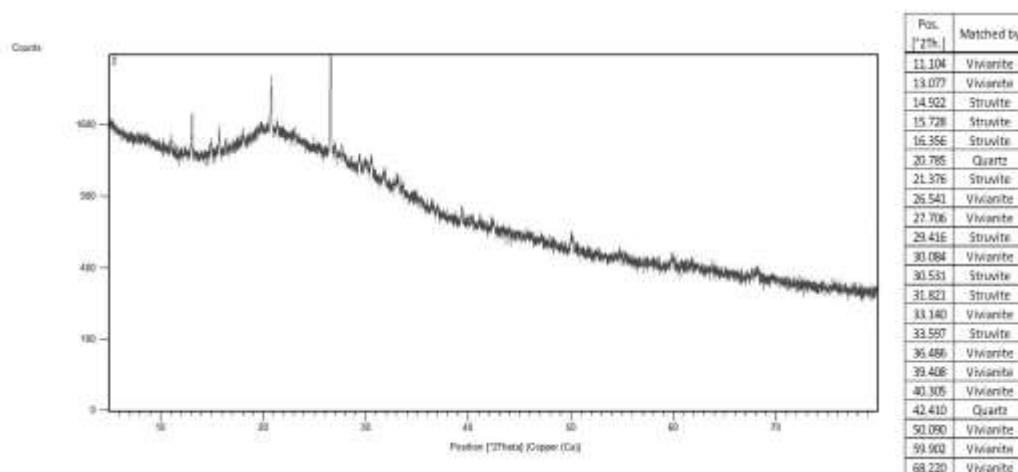
891 *Figure A. 1: XRD diffractogram including peak list and peak assignment for surplus sludge solids sampled*
 892 *in Line 1 (Fe(III) dosing) in Leeuwarden.*



893

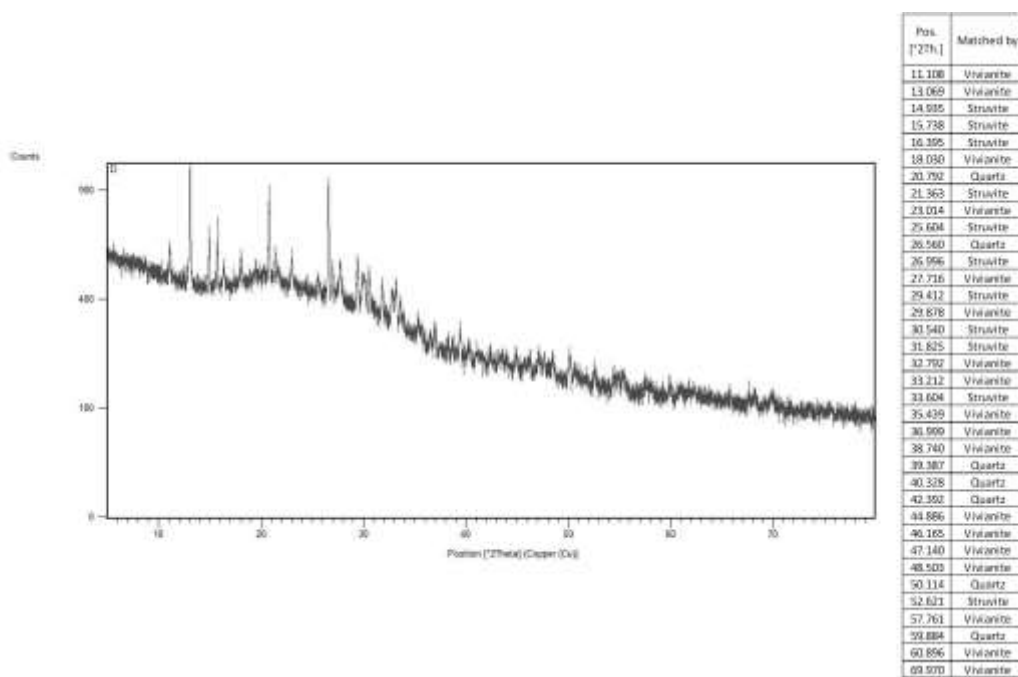
894 *Figure A. 2: XRD diffractogram including peak list and peak assignment for activated sludge solids*
 895 *sampled in Line 2 (Fe(II) dosing) in Leeuwarden.*

896



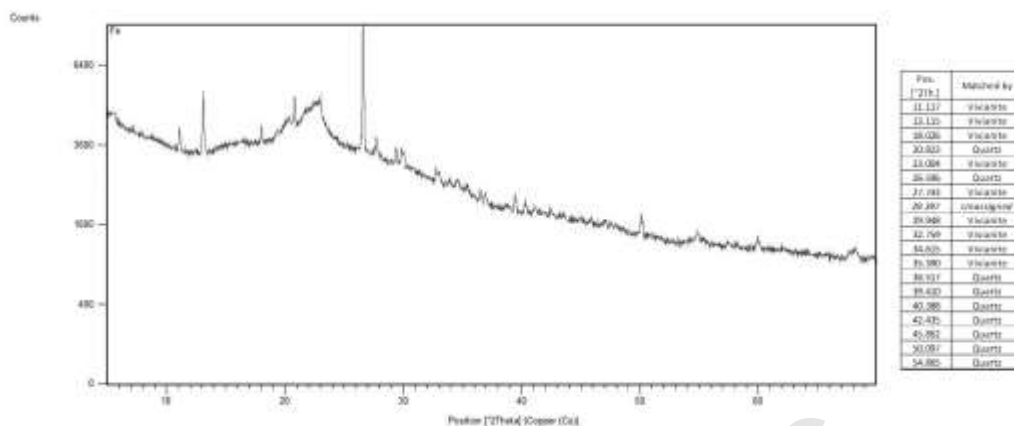
897

898 *Figure A. 3: XRD diffractogram including peak list and peak assignment for surplus sludge solids sampled*
 899 *in Line 2 (Fe(II) dosing) in Leeuwarden.*



900

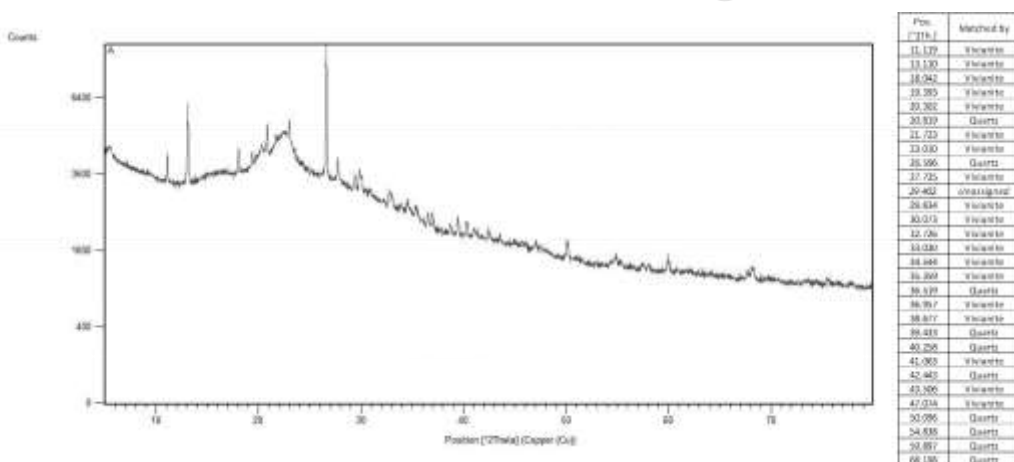
901 *Figure A. 4: XRD diffractogram including peak list and peak assignment for digested sludge solids*
 902 *sampled in Leeuwarden.*



903

904 *Figure A. 5: XRD diffractogram including peak list and peak assignment for A-stage sludge solids sampled*
 905 *directly after Fe(II) dosing in Nieuwveer.*

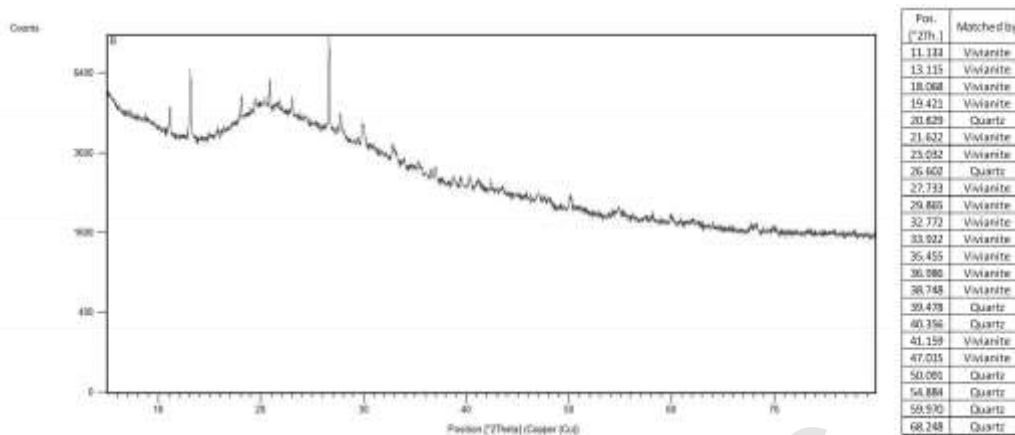
906



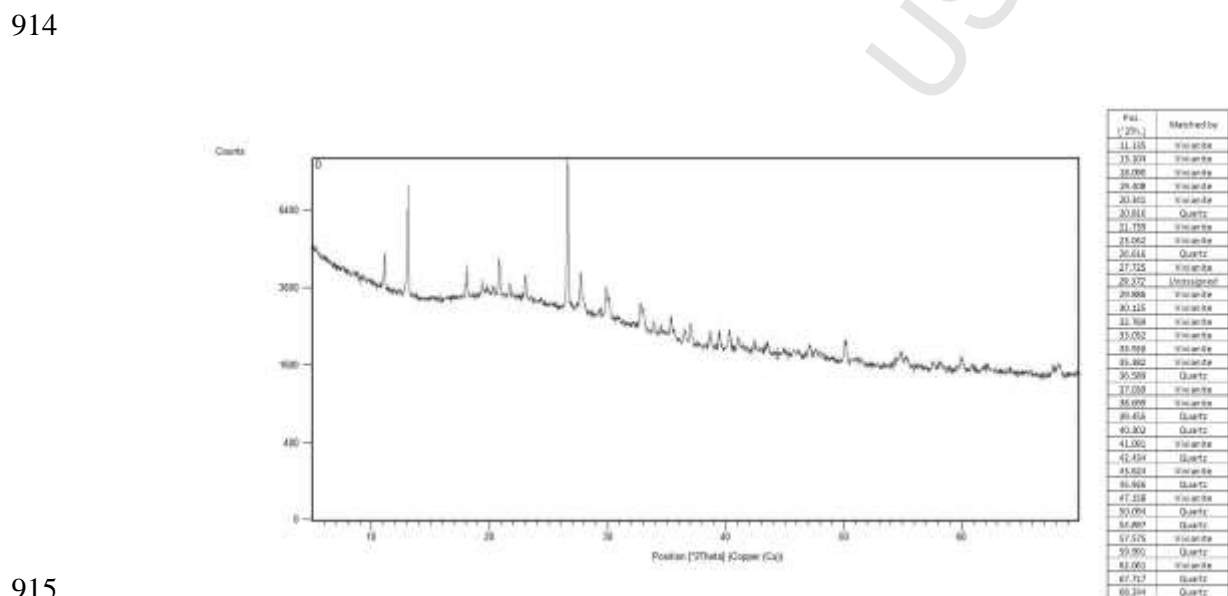
907

908 *Figure A. 6: XRD diffractogram including peak list and peak assignment for surplus A-stage sludge solids*
 909 *sampled in Nieuwveer.*

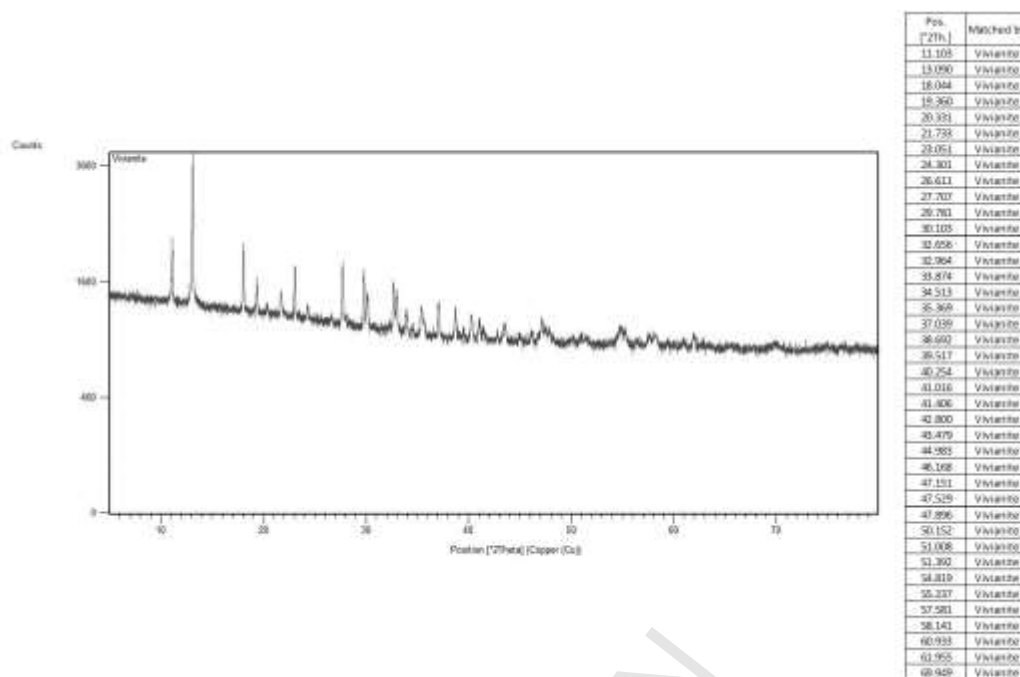
910



911
 912 *Figure A. 7: XRD diffractogram including peak list and peak assignment for surplus B-stage sludge solids*
 913 *sampled in Nieuwveer.*



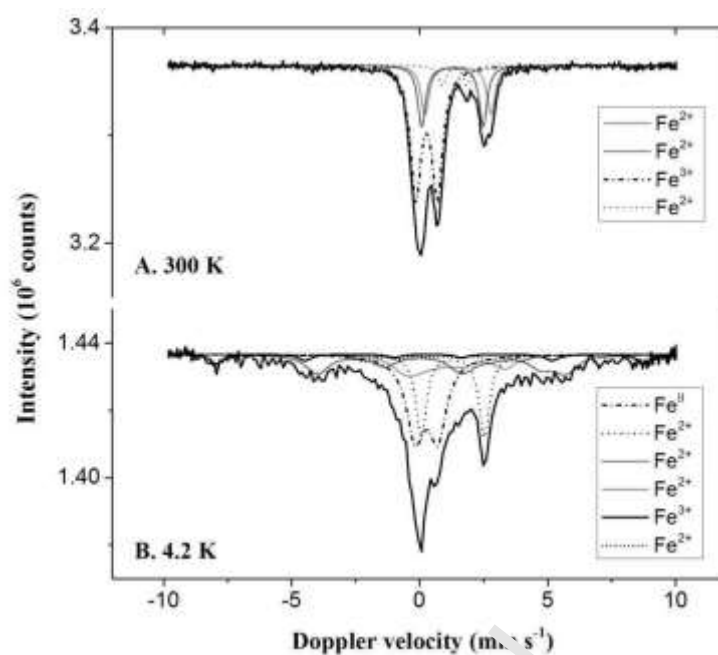
915
 916 *Figure A. 8: XRD diffractogram including peak list and peak assignment for digested sludge solids*
 917 *sampled in Nieuwveer.*



918
919 *Figure A. 9: XRD diffractogram including peak list and peak assignment for the vivianite standard.*

920
921 *Table A. 3: Results of Mössbauer measurements at 300 K.*

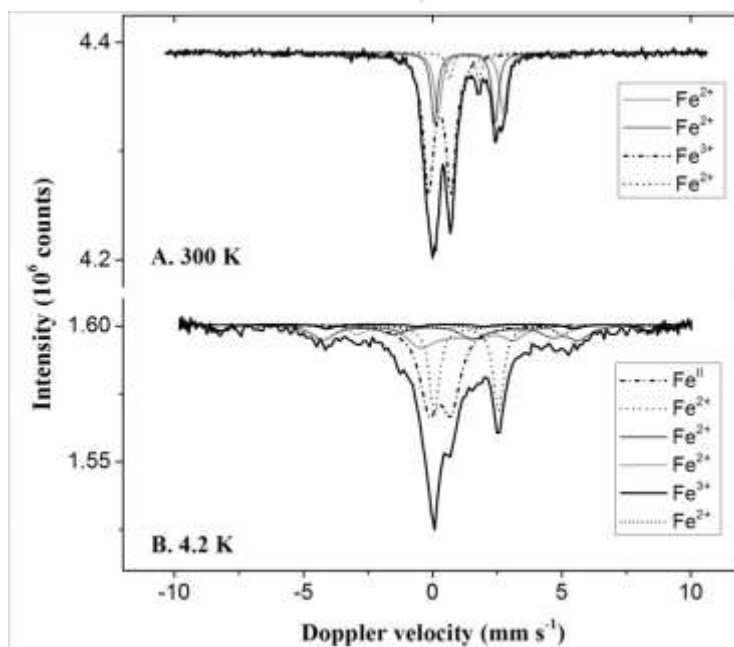
Sample	IS ($\text{mm}\cdot\text{s}^{-1}$)	QS ($\text{mm}\cdot\text{s}^{-1}$)	Hyperfine field (T)	Γ ($\text{mm}\cdot\text{s}^{-1}$)	Phase	Spectral contribution (%)
Leeuwarden Line 1 (Fe(III) dosing)	0.27	0.84	-	0.50	Fe^{3+}	57
	1.28	2.40	-	0.36	Fe^{2+}	20
	1.49	2.58	-	0.38	Fe^{2+}	17
	1.36	0.96	-	0.31	Fe^{2+}	6
Leeuwarden Line 2 (Fe(II) dosing)	0.28	0.87	-	0.49	Fe^{3+}	56
	1.24	2.36	-	0.30	Fe^{2+}	19
	1.47	2.53	-	0.34	Fe^{2+}	18
	1.22	1.13	-	0.28	Fe^{2+}	7
Leeuwarden digested solids	0.27	0.93	-	0.54	Fe^{3+}	62
	1.17	2.46	-	0.32	Fe^{2+}	14
	1.44	2.57	-	0.39	Fe^{2+}	24
Nieuwveer A-stage solids	0.20	0.89	-	0.31	Fe^{3+}	11
	1.08	2.67	-	0.30	Fe^{2+}	33
	1.31	2.74	-	0.34	Fe^{2+}	56
Nieuwveer B-stage solids	0.31	0.85	-	0.48	Fe^{3+}	44
	1.08	2.66	-	0.33	Fe^{2+}	21
	1.39	2.57	-	0.39	Fe^{2+}	35
Nieuwveer digested solids	0.30	0.91	-	0.51	Fe^{3+}	45
	1.07	2.66	-	0.32	Fe^{2+}	19
	1.37	2.64	-	0.39	Fe^{2+}	36
Vivianite Standard	0.23	1.09	-	0.41	Fe^{3+}	20
	1.27	2.33	-	0.42	Fe^{2+}	28
	1.27	2.87	-	0.42	Fe^{2+}	52



922

923 *Figure A. 10: Mössbauer spectra obtained at different temperatures with the surplus sludge solids*
 924 *sampled in Line 1 (Fe(III) dosing) in Leeuwarden.*

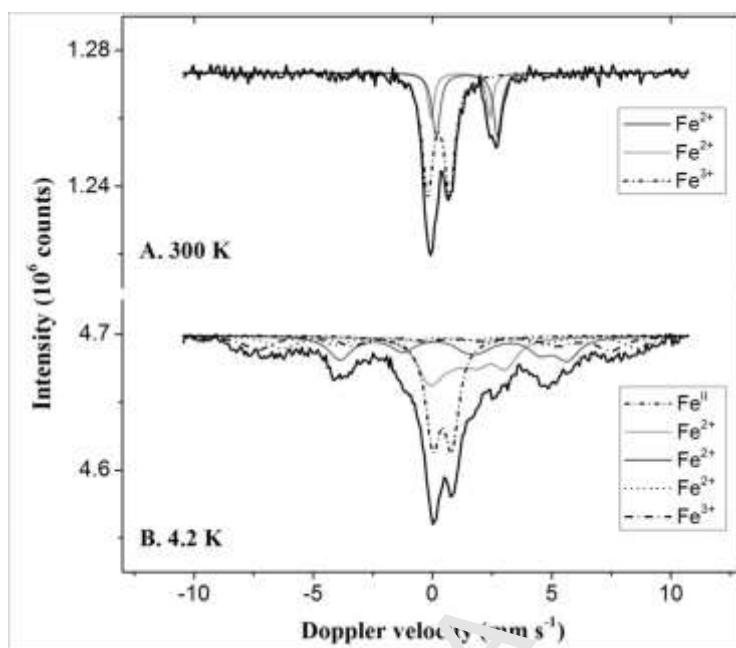
925



926

927 *Figure A. 11: Mössbauer spectra obtained at different temperatures with the surplus sludge solids*
 928 *sampled in Line 2 (Fe(II) dosing) in Leeuwarden.*

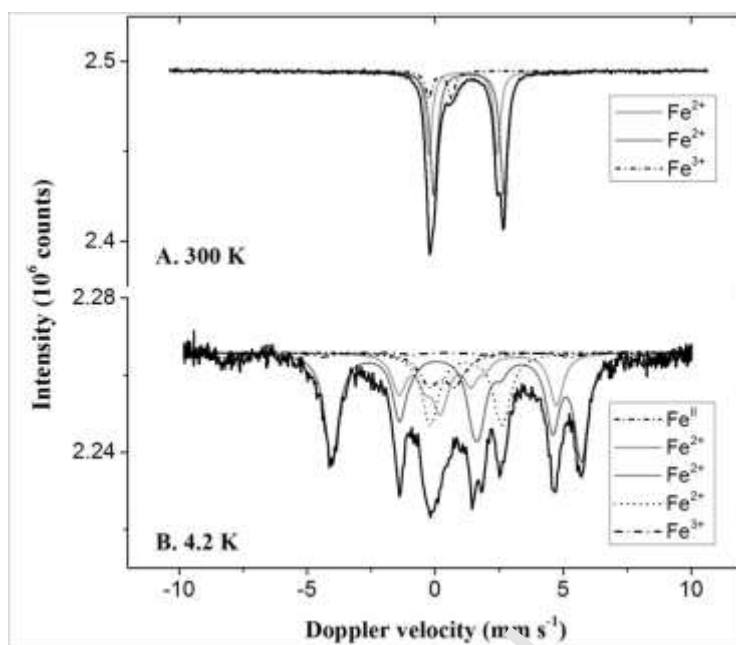
929



930

931 *Figure A. 12: Mössbauer spectra obtained at different temperatures with the digested sludge solids*
932 *sampled in Leeuwarden.*

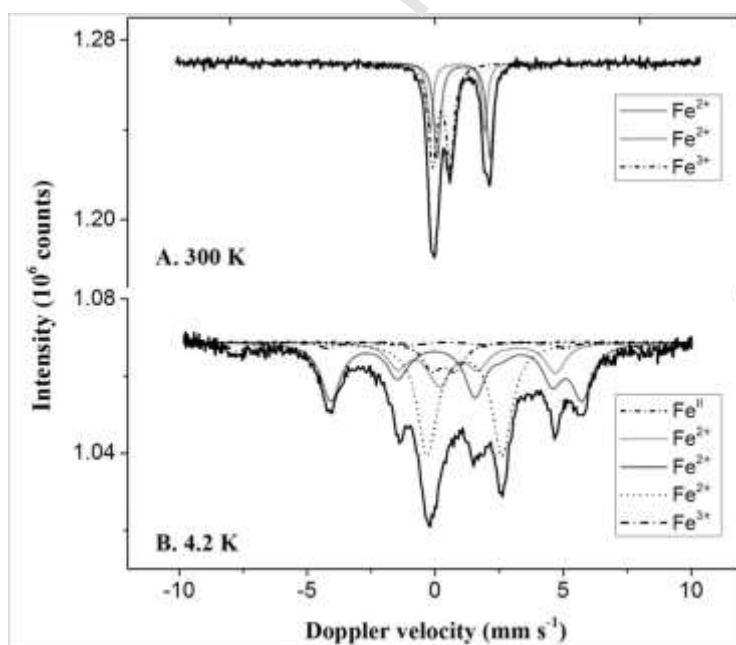
933



934

935 *Figure A. 13: Mössbauer spectra obtained at different temperatures with A-stage sludge solids sampled in*
 936 *Nieuwveer.*

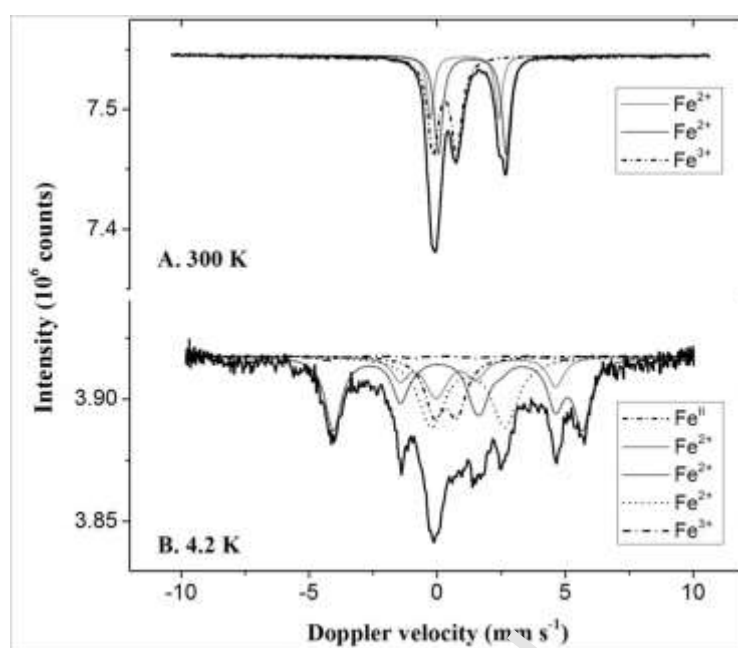
937



938

939 *Figure A. 14: Mössbauer spectra obtained at different temperatures with B-stage sludge solids sampled in*
 940 *Nieuwveer.*

941



942

943 *Figure A. 15: Mössbauer spectra obtained at different temperatures with digested sludge solids sampled*
944 *in Nieuwveer.*

1 Highlights:

- 2 - Fe chemistry and its correlation with P in two sewage treatment plants (STPs) was studied
- 3 - Surplus and digested sludge solids in the investigated STPs were dominated by Fe(II)
- 4 - The Fe(II)P mineral vivianite was a major iron compound in all samples
- 5 - We hypothesize: Vivianite is a key compound in all STPs and offers new P recovery
- 6 routes